

**Compositional Dependence of Physical Properties in  
Nickel-Manganese-Gallium Polycrystals**

By

Christopher Kantner

Submitted to the Department of Materials Science and Engineering in partial  
fulfillment of the requirements for the degree of

Bachelor of Science

at the

Massachusetts Institute of Technology

June 1997

© Massachusetts Institute of Technology 1997. All rights reserved.

Signature of Author. ....

Christopher Kantner  
Department of Materials Science and Engineering  
May 9, 1997

Certified by .....

Robert C. O'Handley  
Senior Research Associate  
Thesis Supervisor

Certified by ... ..

August F. Witt  
Ford Professor of Engineering  
Thesis Supervisor

Accepted by .....

David K. Roylance  
Chairman, Undergraduate Thesis Committee

MASSACHUSETTS  
INSTITUTE OF TECHNOLOGY

DEC 24 1997

ARCHIVES

LIBRARIES

## **Acknowledgments**

I would like to thank Dr. Bob O'Handley for being my thesis advisor and providing support throughout the term on this project. His assistance was beneficial and it has been a pleasure working for him.

I would also like to thank the rest of the group, especially Jiankang Huang. Without his help with the magnetostriction measurements, I would never have finished this thesis. Thanks to Doug Matson and John Lum for giving me access to the induction melting facilities. I also need to thank Neel Chatterjee for the EPMA measurements.

Finally, I would like to thank Professor Witt for agreeing to be my co-advisor so late in the term.

# **Compositional Dependence of Physical Properties in Nickel-Manganese-Gallium Polycrystals**

By

**Christopher Kantner**

Submitted to the Department of Materials Science and Engineering on May 9, 1997 in  
partial fulfillment of the requirements for the degree of  
Bachelor of Science.

## **Abstract**

My thesis examined the compositional dependence of physical properties in nickel-manganese-gallium alloys. The properties examined were magnetization, martensite transformation temperature, Curie temperature, and magnetostriction. Magnetization in a field of 10 kOe was found to vary from 0.5 emu/gram in paramagnetic samples to 50 emu/gram. The martensite transformation temperature varied from below -75 °C to 43 °C. The Curie temperature was found to vary between 45 °C and 80 °C. Magnetostriction was only measured on four samples and only one sample showed magnetostriction. One sample showed a strain of 300 ppm in a field of 6 kOe.

Thesis Supervisor: Dr. Robert C. O'Handley  
Title: Senior Research Associate

Thesis Supervisor: August F. Witt  
Title: Ford Professor of Engineering

## **Table of Contents**

1. Introduction	page 6
2. Literature Survey	page 13
3. Experimental Procedure	page 19
4. Results	page 22
5. Discussion	page 29
6. Conclusions	page 34
References	page 36
Appendix A	page 37
Appendix B	page 44

# List of Figures and Tables

## Figures

1.1 Activation of twin boundary motion.	page 9
2.1 Crystal Structure of Ni <sub>2</sub> MnGa.	page 13
2.2 Magnetic field induced strain of single crystal.	page 14
2.3 Magnetization vs. field in austenitic and martensitic phases of single crystal.	page 15
2.4 Magnetization vs. temperature in many magnetic fields.	page 16
2.5 Magnetization vs. temperature and DSC curves.	page 17
4.1 Projected sample compositions.	page 22
4.2 Actual sample compositions.	page 23
4.3 Magnetization vs. field of an austenite sample	page 23
4.4 Magnetization vs. field of a martensite sample.	page 24
4.5 Magnetization vs. field of a paramagnetic sample.	page 24
4.6 Magnetization vs. temperature showing Curie temperature.	page 25
4.7 Magnetization vs. temperature showing martensite and Curie temperatures.	page 25
4.8 Magnetostriction in martensite phase of sample 1.	page 26
4.9 Magnetostriction in austenite phase of sample 1.	page 27
5.1 Magnetization as a function of composition.	page 30
5.2 Martensite temperature as a function of composition.	page 31
5.3 Curie temperature as a function of composition.	page 32

## Table

Table 1. Summary of sample properties.	page 28
--	---------

# **Chapter 1**

## **Introduction**

Shape memory alloys have the unique property of being able to exhibit large, recoverable strains because deformation occurs by twin boundary motion. This large strain can be exploited to do useful work in a device. One example of such a device is an actuator.

Actuators are devices that provide motion and force in order to control mechanical behavior [1]. Combining actuator materials with sensing equipment makes it possible to fabricate a device that is able to sense and adapt to its surroundings. This device makes it possible for a machine to sense its environment and adapt itself in order for the machine to maximize a given property, such as efficiency, in that environment. One specific example of a potential use of actuators is in the rollers of a steel or paper mill. The output of the mill is limited by the vibrations of the rollers about its neutral axis. Sensors and actuators could be placed around the axle of the rollers and sense the vibrations and then react to dampen the vibrations so the efficiency of the mill would be maximized.

For such a device to work, two different systems must be integrated together. A sense and control system is one part of the device and the second part is the actual actuator. The actuator could be a motor or other driver or it could be an actuator material. The advantage of using a material instead of a machine are that a material is simpler and can be more efficient. The actuator material is the part of the device that does the actual work. The search for new actuator materials combining larger stroke and rapid frequency response is a current interest in materials science.

Finding the new actuator material is not a simple task because of the many properties that must be optimized. The material must produce a large strain when activated and deliver a large force to be useful for doing work. The material should also be able to respond rapidly to the activating signal so the applications of the device will not be limited by the frequency response of actuator material. Another issue is the energy efficiency of the actuator material. Energy conversion efficiency should be optimized so the overall productivity of the device makes it practical for use in machinery. One final consideration for the actuator material is cost. The cost of the device has three components. The initial cost involves the materials cost, processing cost, labor, packaging, research and development, and marketing. The second cost involves the cost of use which is directly related to power efficiency. The final cost is in the disposal and recycling of the material. Ideally, all of the properties should be optimized and the cost of the actuator material should be small. This makes an actuator material cost effective

Currently, there are three major classes of actuator materials available for devices. These are piezoelectric ceramics, magnetostrictive metals, and shape memory alloys [1].

Each of these materials has an array of advantages and disadvantages. No one class of material dominates the current actuator market.

Piezoelectric ceramics strain under the application of an electric field. Because they are insulators, the frequency response can be very rapid, but metals can not respond as quickly as piezoelectric materials. However, the strains resulting from the electric field are very small so the amount of work a piezoelectric actuator can do is limited.

Magnetostrictive materials are materials that strain under the application of a magnetic field. These materials have strains that are somewhat larger than those of piezoelectric materials and they have an adequate frequency response because the external magnetic field can be changed rapidly. However, the strains resulting from magnetostriction are only marginally adequate for vibration suppression. Another factor that hinders the use of magnetostrictive materials is their cost. Terfenol-D [2], the current industry standard, is very expensive because it is composed of the rare earth elements terbium and dysprosium in addition to iron. Another problem with Terfenol-D is that it is prone to corrosion.

The third class of materials are shape memory alloys. These materials exhibit very large strains so they are capable of performing large amounts of work. However, the current shape memory effect is controlled by heating and cooling the material through the martensite transformation temperature. This is called thermoelastic behavior. Controlling material temperature is much slower than controlling an external electric or magnetic field so the frequency response of these materials is very poor compared to the other classes of materials. In addition, temperature changes lead to excess heat loss and, therefore, lower efficiency.



Currently, all of the desired properties are represented in one of these actuator materials but no one material possess all of the needed characteristics. Research on a new type of material is showing the potential of one material to possess all of the needed features of an ideal actuator. This class of materials uses a magnetically driven shape memory effect instead of the normal thermoelastic shape memory effect. These magnetic shape memory materials will combine the large strains associated with normal shape memory alloys and have the rapid response that is associated with magnetostrictive materials because the materials will be controlled by an external magnetic field [2].

Magnetically driven shape memory alloys differ from thermoelastic shape memory alloys because the magnetic shape memory alloys can operate fully in the low temperature phase. The large, recoverable strains are caused by magnetic field driven motion of twin boundaries in the martensite phase. Once a magnetic field is applied, twin variants with a magnetization orientation that gives a favorable energy in the applied field will grow consuming the twins with less favorable energy.

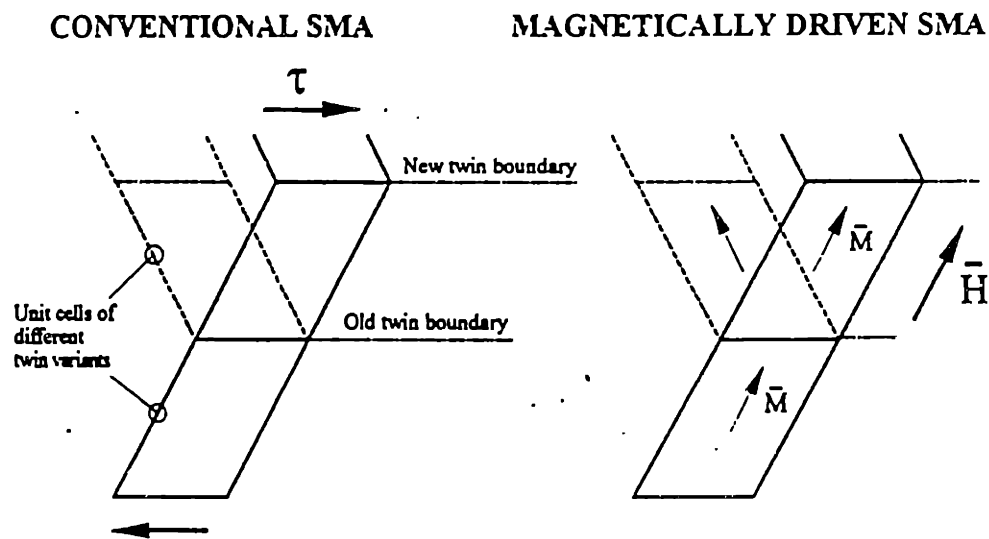


Figure 1.1  
Activation of twin boundary motion

This causes the material to strain. Two criteria must be met by the material if it is to be a magnetically driven shape memory alloy. First, the material must have a high magnetic anisotropy energy. This means that magnetization will lie along one crystal axis almost exclusively. If this is the case, the twin variants not aligned with the field will be reduced in size by the twin boundary motion. If the material has low anisotropy energy, the external magnetic field would turn the magnetization onto another axis in the crystal instead of actually moving the twin boundaries. If the unfavorable twin variants are not shrunk by the field, the desired strain will not be achieved. Second, the material must have low twin boundary motion energy. The strain in these materials depends on the motion of twin boundaries so if the energy of twin boundary motion is too high, the boundaries will not move and the material will not have the desired properties.

These materials have the potential to dominate some segments of the actuator market because of their unique properties. These materials combine the large strain from the shape memory effect with the rapid response of piezoelectric materials or magnetostrictive materials so they would be very attractive to the actuator industry. Unfortunately, there has not been a magnetic shape memory material that has been optimized for use as a magnetically driven actuator. However, research is being done to find a material that will perform adequately in a commercial device.

So far, the impressive potential of magnetic shape memory alloys has been shown in single crystals of  $\text{Ni}_2\text{MnGa}$ . This thesis will further examine the prospects of  $\text{Ni}_2\text{MnGa}$  for use as a magnetic shape memory actuator material. The material must exhibit a martensite transformation temperature near or above room temperature because the magnetic shape memory effect occurs in the martensite phase. The martensite

transformation temperature of the material must be near room temperature for the material to be of practical use in devices. The material must also possess a strong magnetization if it is to do work. The force the material can deliver is related to the magnetization. Work is a function of force and distance so an ideal material will be capable of large forces and large strains. Another factor that must be accounted for is the Curie temperature. Above the Curie temperature, the material will lose its long range magnetic order and, therefore, not be capable of producing a force. The temperature of operation of the material must not exceed the Curie temperature of the material or else the material will fail. A final characteristic that will be examined is how the crystal structure of the material affects the performance. The potential for Ni<sub>2</sub>MnGa was shown in single crystals but this research will be performed on polycrystalline samples.

This thesis studied how critical properties vary with composition in polycrystalline samples of Ni<sub>2</sub>MnGa. The properties that were examined are: Martensite transformation temperature, Curie temperature, magnetization, and magnetically induced strain. The study was done by starting with a base composition and producing samples that hold the fraction of one component constant while varying the other two. Three series of samples were produced, each series keeping one of the elements at a constant atomic percent.

This thesis will work to establish the effect of composition on material properties. By determining how the properties change with composition, it will be possible to predict the compositions that will be useful in devices. This project also examined the effectiveness of polycrystalline samples as opposed to single crystals. Currently, the only work has dealt with single crystals. The strains exhibited in this project will establish the effectiveness or ineffectiveness of polycrystalline samples. This information will steer

further research towards or away from single crystals. This project will help determine the material that could be used in devices in the future.

## Chapter 2

### Literature Survey

$\text{Ni}_2\text{MnGa}$  is a Heusler alloy having a cubic structure when in the austenitic phase.

The lattice constant is 5.822 angstroms[3].

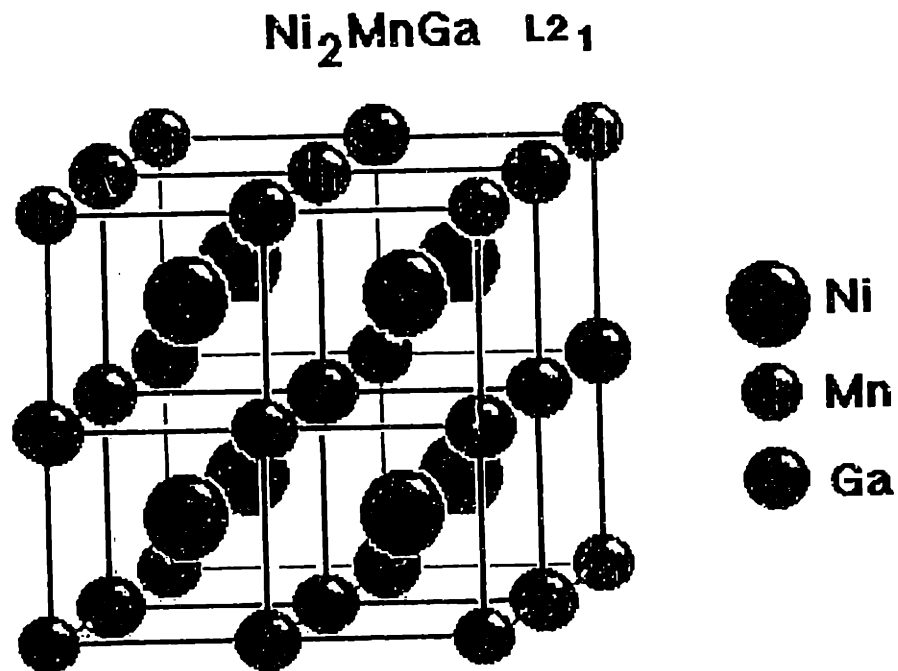


Figure 2.1  
Crystal structure of  $\text{Ni}_2\text{MnGa}$

The martensite phase is a tetragonal structure with lattice parameters  $a$  and  $b$  equal to 5.90 Å and  $c$  axis has a lattice parameter of 5.44 Å. The strain associated with the

transformation from austenite to martensite (-6.56% along the c axis) is accommodated by the formation of twin variants. The formation of twin variants acts to minimize the strain energy that accompanies the transformation of phases. Because the transformation from austenite to martensite causes twin variants to form, Ni<sub>2</sub>MnGa is a possible material for use as a magnetic shape memory alloy. In fact, large strains have been achieved at 77 K by applying stresses of 2 Mpa. A recoverable strain of 5% has been attained when stressing in the [100] direction [4].

Large magnetic-field-induced strains have been seen in single crystals[5]. The single crystal had a martensite transformation temperatures on cooling and heating of 276 K 281.5 K, respectively. This shows that the sample exhibits a thermal hysteresis. A strain of nearly 0.2 % has been achieved in a field of 8 kOe.

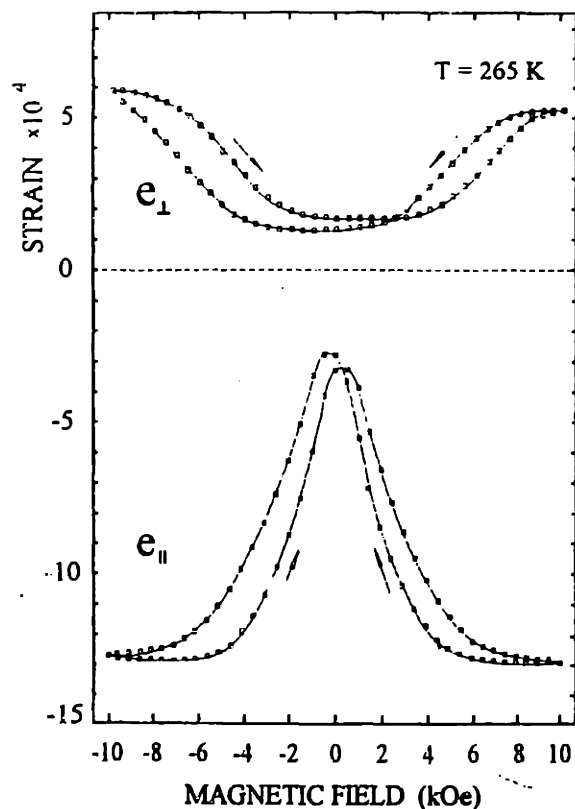


Figure 2.2  
Magnetic field induced strain of single crystal[5].

At the time, this was the largest magnetic-field-induced strain in non-rare-earth materials in fields below 10 kOe [5].

The magnetization of the single crystal sample is different in the martensite and austenite phases. The magnetization of the austenite phase saturates to a value of approximately 47 emu per gram in a field under 2 kOe while the martensite phase saturates to a value of approximately 58 emu per gram in a field of 8 kOe.

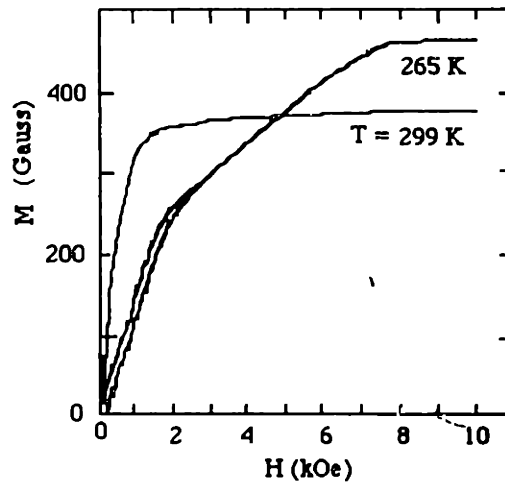


Figure 2.3  
Magnetization vs. field in austenitic and martensitic phases of single crystal[5].

The reason for the different fields needed to saturate the magnetization is the difference in crystal structure and, hence, the difference in magneto-crystalline anisotropy. These values are significantly lower than those reported by Webster et. al. However, the martensite temperature of the sample examined by Webster et. al. had a martensite transformation temperature of 202 K and it did not show thermal hysteresis.

Both of the above groups used magnetization vs. temperature measurements to determine the martensite transformation temperature. At low fields, there is a discontinuous change in magnetization.

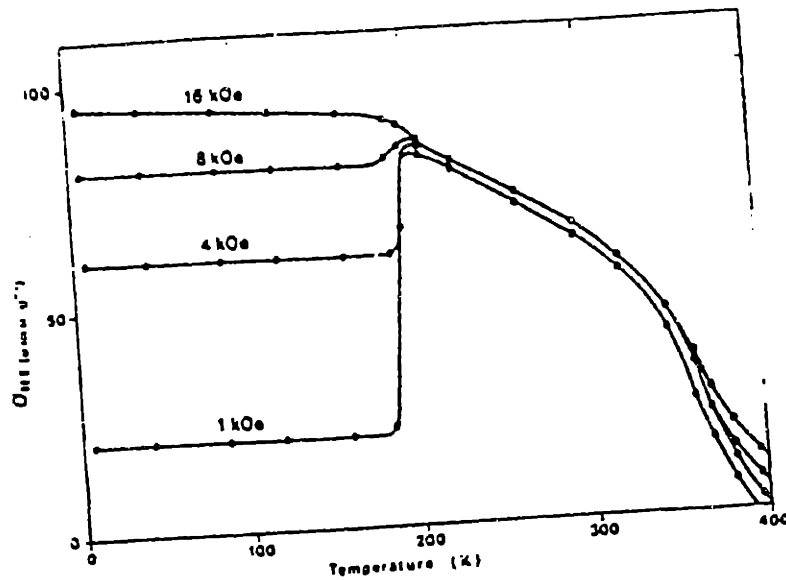


Figure 2.4  
Magnetization vs. Temperature in many magnetic fields[3].

This is the result of the twin variant formation. The magnetization of the martensite is lower because there are fewer twin variants having their magnetic easy axes aligned in the field. This also explains why the martensite phase is much harder to saturate than the austenite phase.

One group has examined how the martensite transformation temperature and Curie temperature vary with composition[6]. They examined 23 samples of  $\text{Ni}_2\text{MnGa}$ . The group used differential scanning calorimetry and low field magnetic susceptibility to measure martensite transformation temperatures. The temperatures scanned varied from 4.2 K to 890 K. Martensite transformation temperatures were found to vary from 113 K to 626 K. Two samples did not show a martensite transformation in the temperature range scanned. The martensite transformation temperature is assumed to be below 4.2 K for these two samples. The Curie temperatures varied from 341 K to 387 K. Chernenko



et. al. did not examine magnetization of their samples. Low field magnetic susceptibility measurements showed a martensite transformation at one temperature while differential scanning calorimetry showed a different transformation temperature for the same sample, as is shown in figure.

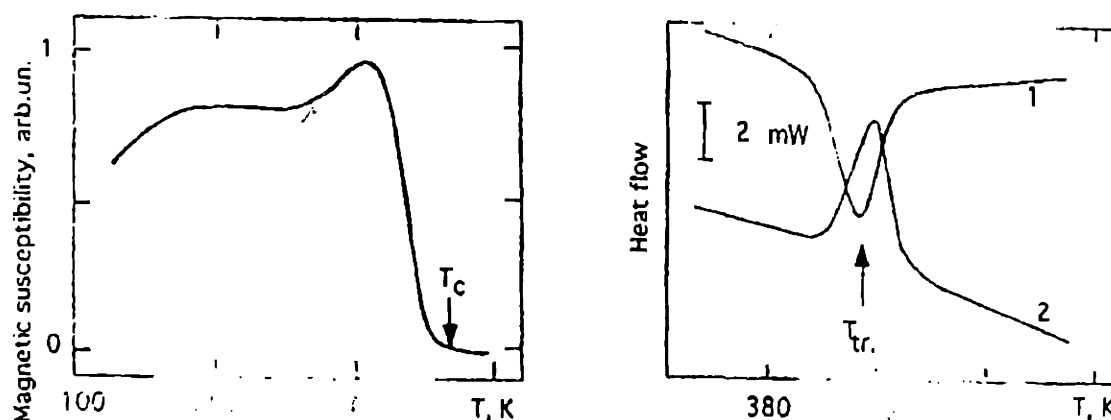


Figure 2.5  
Magnetization vs. temperature and DSC curves[6].

The martensite transformation is believed to occur at the point where there is a discontinuous jump in magnetization [3] so the results that were obtained from differential scanning calorimetry may differ from those obtained by magnetic measurements.

So far, only single crystal samples have shown the large field magnetic field induced strain measurements. The other papers on  $\text{Ni}_2\text{MnGa}$  did not examine how the samples strain when subjected to a magnetic field. Because of the discrepancies in  $T_M$  values suggested by various methods, it was decided to conduct an independent study of the physical properties of nickel-manganese-gallium shape memory alloys.

A second system of materials has exhibited behavior similar to that found in nickel-manganese-gallium. The system is iron-palladium. Large magnetic field induced strains are possible when this system is in its martensitic phase. Strains of nearly 0.5% have been achieved in these samples at a temperature of -36 °C [7]. This is larger than that achieved in single crystals of nickel-manganese-gallium, but, the larger strain was achieved at a lower temperature.

## **Chapter 3**

### **Experimental Procedure**

#### **A. Sample Preparation**

Sixteen samples, each weighing approximately 12 grams, were prepared by induction melting of the appropriate quantities of the starting elements. The purity of the starting elements were 99.9% for nickel, 99.98% for manganese, and 99.99999% for gallium. The samples were melted using a Lepell induction melting apparatus. The raw materials were kept in the induction field until it appeared that the entire sample was molten. This occurred near 1300 °C. Care was taken to not overheat the samples so there would not be a large loss of high vapor pressure material, such as gallium and manganese. Argon gas was flowed over the samples to reduce oxidation of the samples at the high temperatures. The samples were allowed to cool in the presence of the argon gas flow. Weight loss of the samples was less than 1%. The ingots were then vacuum encapsulated in quartz and back-filled with argon gas. Tantalum was included in the capsules to act as a gettering agent. Care was taken to ensure the tantalum was not in contact with any of the ingots. The samples were heat treated at 1000 °C for 24 hours to ensure homogenization

and then the temperature was lowered to 700 °C and the samples were kept at that temperature for another 24 hours to optimize ordering. The ordering temperature is 810 °C. The capsules were quenched in water after the heat treatment was finished. The ingots were cut using a low speed diamond saw to produce pieces for further study.

### **B. Compositional Analysis**

The composition of the samples were determined using electron probe micro-analysis (EPMA). The compositions of the samples were expected to differ from the projected compositions because gallium and manganese have high vapor pressures and it was difficult to control the temperature the samples were heated to during melting. Two points were chosen at random on the surface of the samples to determine the composition. The composition of the samples was taken to be the average of the points analyzed. Only two points were analyzed on the samples because of the consistency of the results and analysis of further points was deemed unnecessary. Some samples showed macro-phase separation and were discarded from the study.

### **C. Magnetic Tests**

Magnetization versus field tests were performed on all samples using a vibrating sample magnetometer. The field was varied from 10 kOe to -10 kOe in 500 Oe steps. These tests were done to determine the saturation magnetization of the samples, the magnetic anisotropy field needed to reach saturation, and the coercivity. Magnetization versus temperature tests were then done to determine martensite transformation temperature and Curie temperature. The magnetization versus temperature was measured in a field of 500 Oe over the temperature range of -75 °C to 75 °C in 5 °C increments. After this initial test, further magnetization versus temperature measurements were taken

if a martensite transformation was seen in the temperature range previously tested. The second tests examined the region from the martensite transformation temperature to the Curie temperature in 1 °C increments.

# Chapter 4

## Results

Figure 4.1 shows the compositions of the elements weighed before melting. Figure 4.2 shows the average composition of the samples, as determined by EPMA after melting and annealing.

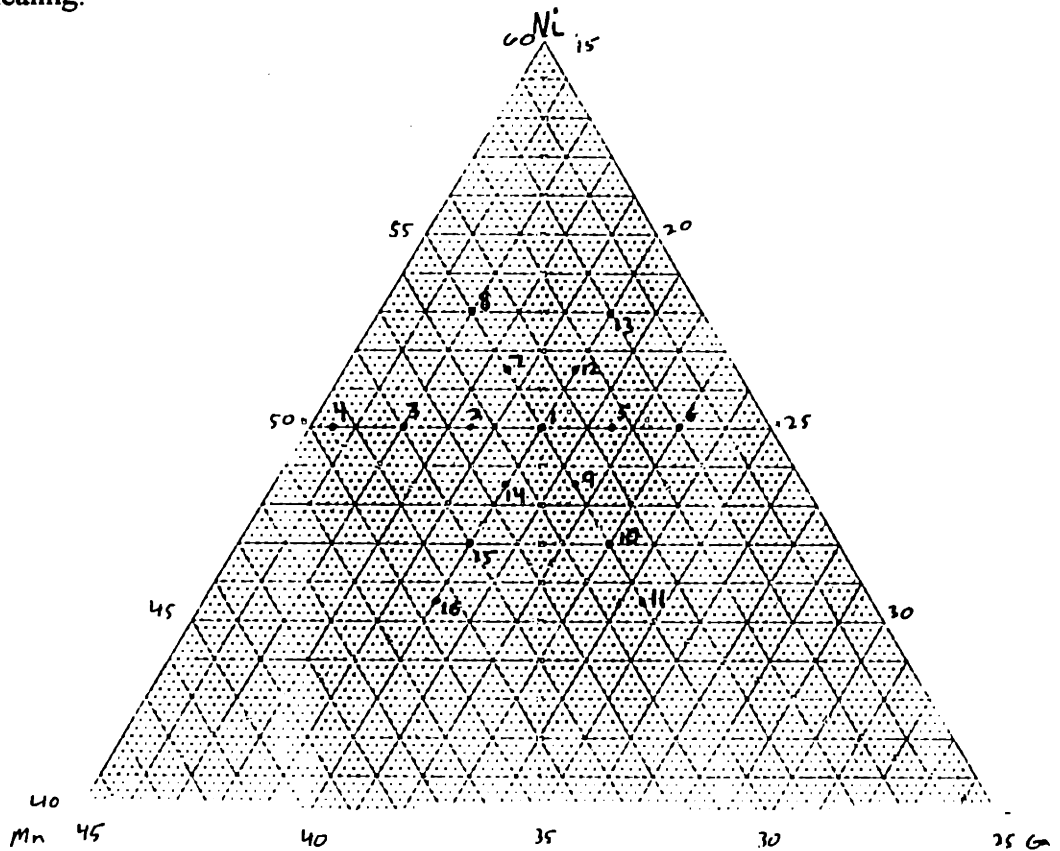


Figure 4.1  
Projected sample compositions

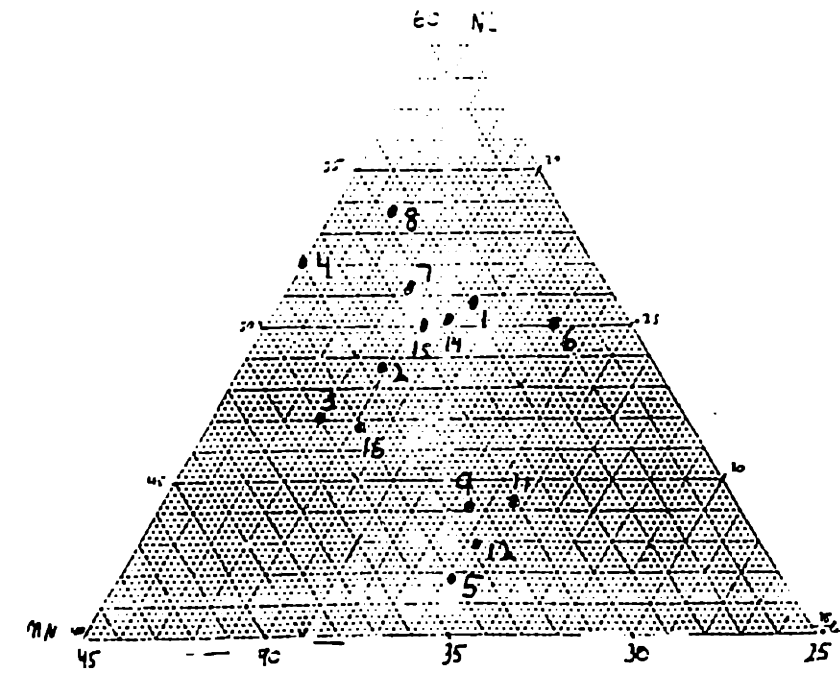


Figure 4.2  
Actual sample compositions

Samples 10 and 13 were found to be inhomogeneous on the surface examined by EPMA so these samples were not tested. Figures 4.3-4.5 show examples the room temperature magnetization vs. field curves for the 14 samples that were found to be homogeneous. Curves for all samples can be found in appendix A.

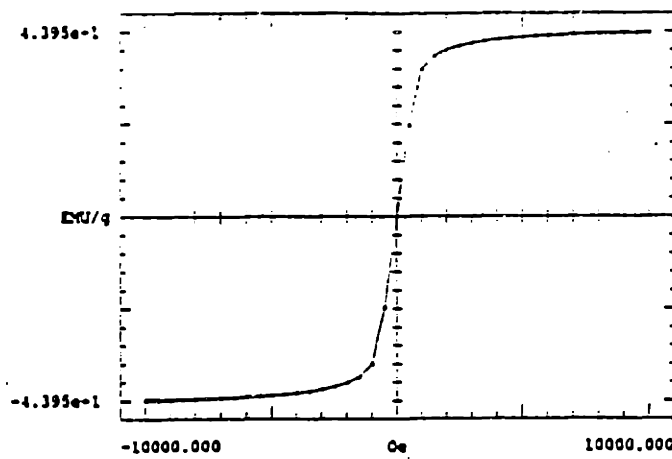


Figure 4.3  
Magnetization vs. field of an austenite sample.

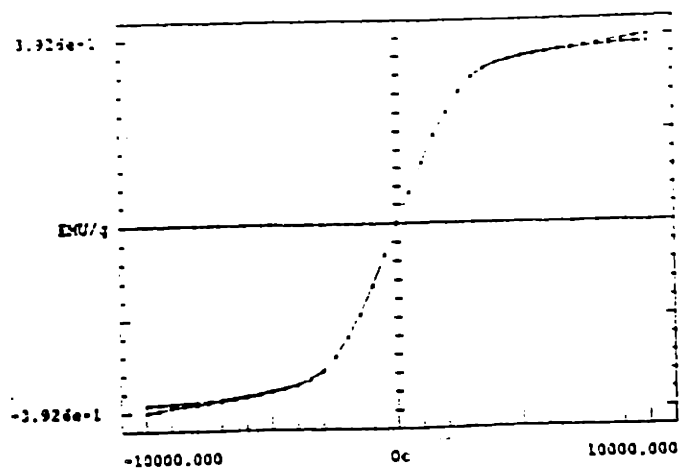


Figure 4.4

Magnetization vs. field of a martensite sample.

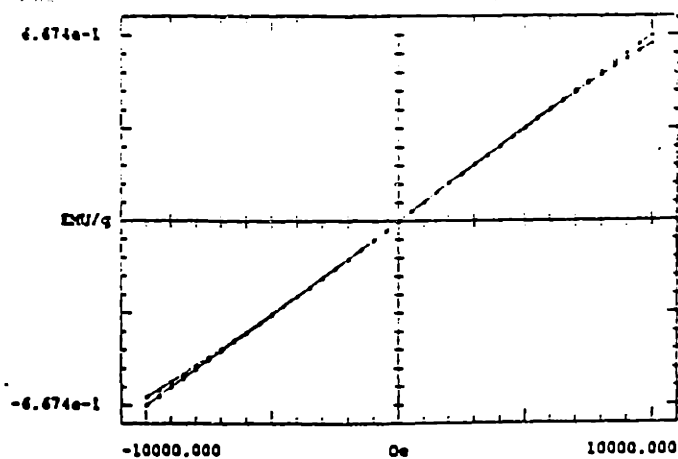


Figure 4.5

Magnetization vs. field of a paramagnetic sample.

Three types of curves are displayed by the samples. The curves that reach the saturation magnetization easily,  $H_{sat} < 1000$  Oe, are those of austenite phases. The curves that are sheared over,  $H_{sat} > 2000$  Oe, are samples in the martensite phase. The curves which are linear are samples that are paramagnetic. The magnetization at 10 kOe varies from approximately 0.5 emu/gram to 50 emu/gram between the samples. The saturation magnetization of metallic nickel is 56 emu/gram.



Examples of magnetization vs. temperature curves are shown in figures 4.6 and 4.7. M vs. T curves for all samples can be found in appendix B.

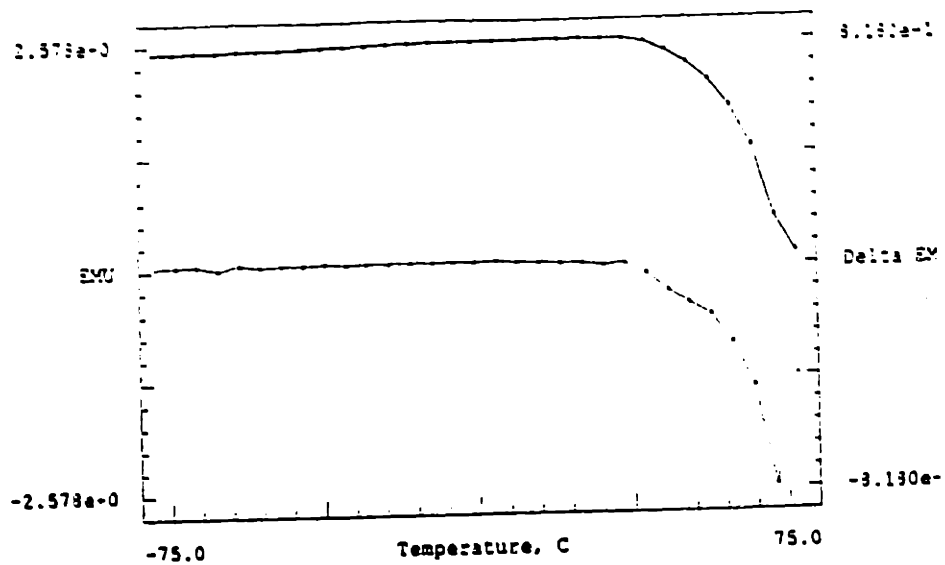


Figure 4.6  
Magnetization vs. temperature showing Curie temperature.

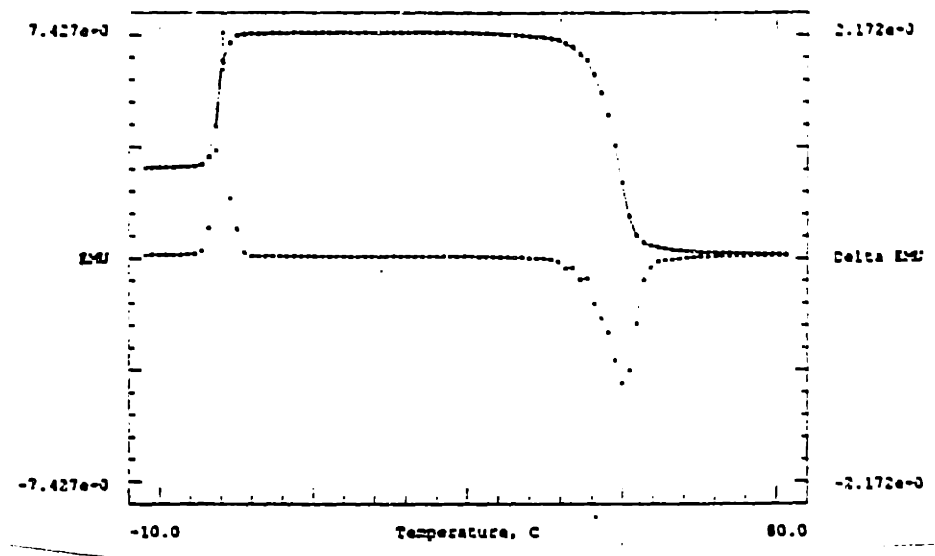


Figure 4.7  
Magnetization vs. temperature showing martensite transformation and Curie temperature.

The Curie temperature is the temperature above which magnetization vanishes. The martensite temperature is the temperature below which it is harder to saturate the sample. So the magnetization at 500 Oe drops sharply at the martensite temperature. The martensite transformation temperature can be seen on some of these curves and the Curie temperature can be seen on all of the curves. Some of the samples do not show the martensite transformation because the transformation temperature is out of the temperature range examined.

Strain measurements were performed on the samples that had a martensite transformation temperature near room temperature. Four samples exhibited transformation temperatures near room temperature. Magnetostrictive strain measurements were performed at 0 °C to ensure that the samples were fully martensite. Two samples showed moderate strains in the applied magnetic field while two samples did not show any magnetostriction. Figures 4.8 and 4.9 show magnetostrictive strains in sample 1 in the martensite phase and the austenite phase.

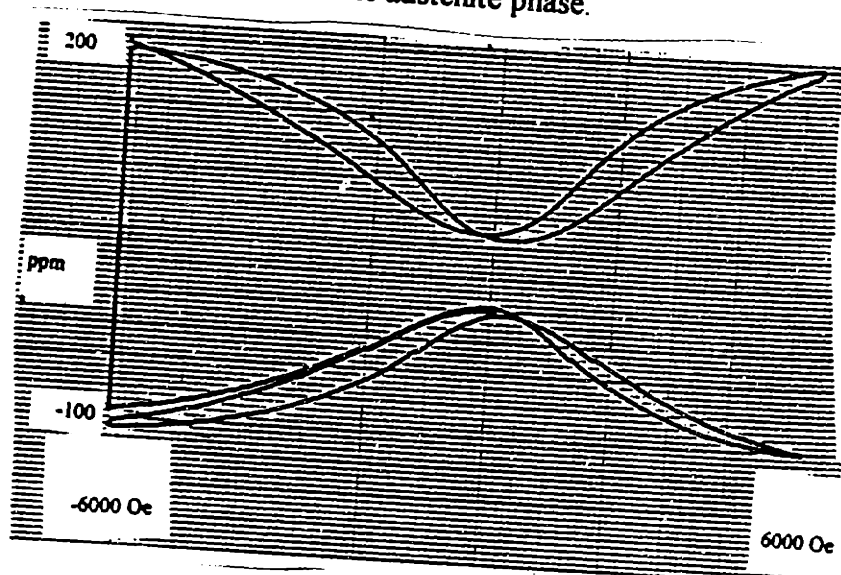


Figure 4.8  
Magnetostriction in martensite phase of sample 1.

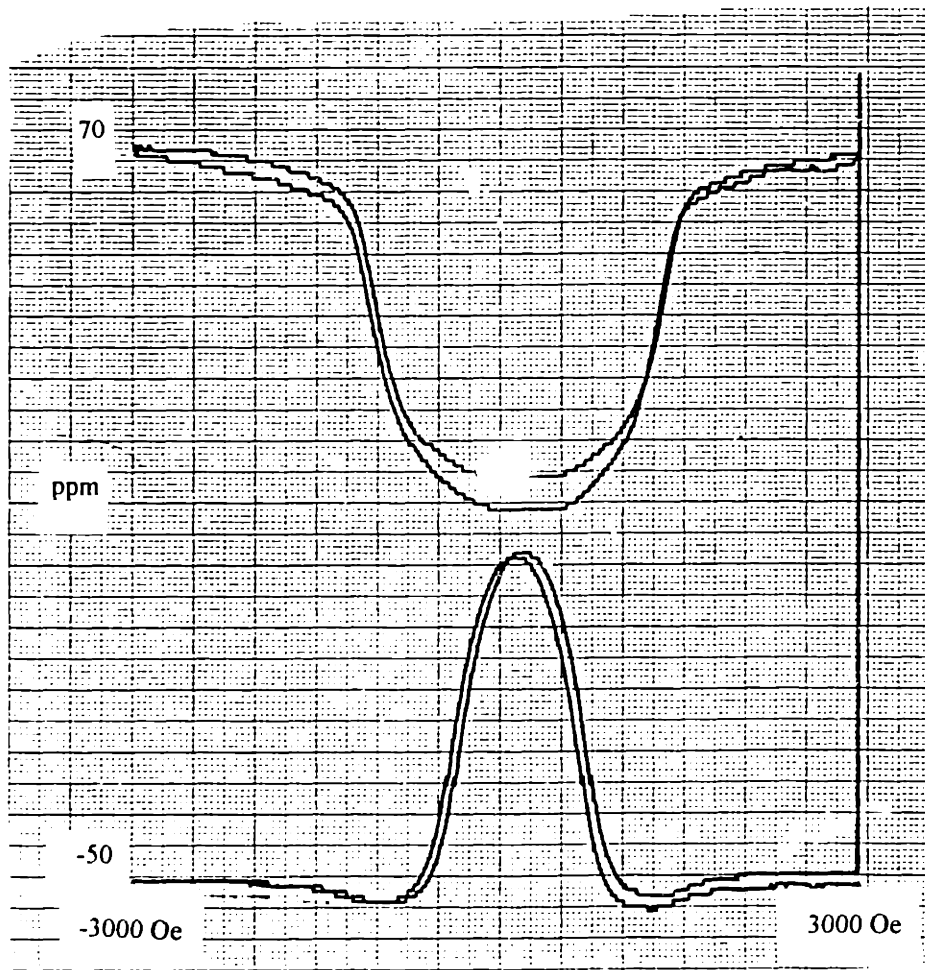


Figure 4.9

Magnetostriction in austenite phase of sample 1.

A negative strain is observed when the field is aligned parallel with the strain gage a positive strain is observed when the field is applied perpendicular to the strain gage. The maximum strain is the difference between the two strain values. Sample 14 exhibited a small amount of magnetostriction. Samples 2 and 16 were also tested but failed to show any magnetostriction. Table 1 gives a summary of the results from the tests performed on all samples.

Sample	Composition	Saturation Magnetization (Emu/gram)	Martensite Transformation Temperature (°C)	Curie Temperature (°C)
1	Ni <sub>50.7</sub> Mn <sub>29</sub> Ga <sub>20.3</sub>	50.346	12	70
2	Ni <sub>48.6</sub> Mn <sub>32.6</sub> Ga <sub>18.8</sub>	16.757	42	51
3	Ni <sub>47.1</sub> Mn <sub>35.1</sub> Ga <sub>17.8</sub>	9.0257	?	47
4	Ni <sub>52</sub> Mn <sub>33.1</sub> Ga <sub>14.9</sub>	.57054	-----	-----
5	Ni <sub>41.7</sub> Mn <sub>34.1</sub> Ga <sub>24.2</sub>	24.315	< -75	80
6	Ni <sub>50</sub> Mn <sub>27.2</sub> Ga <sub>22.8</sub>	45.428	-80	66
7	Ni <sub>51.1</sub> Mn <sub>30.5</sub> Ga <sub>18.4</sub>	20.521	?	45
8	Ni <sub>53.7</sub> Mn <sub>29.7</sub> Ga <sub>16.6</sub>	.65174	-----	-----
9	Ni <sub>44.2</sub> Mn <sub>32.3</sub> Ga <sub>23.5</sub>	43.810	< -75	75
11	Ni <sub>44.2</sub> Mn <sub>31.1</sub> Ga <sub>24.7</sub>	32.816	< -75	70
12	Ni <sub>42.9</sub> Mn <sub>32.8</sub> Ga <sub>24.3</sub>	27.044	< -75	75
14	Ni <sub>50.2</sub> Mn <sub>30</sub> Ga <sub>19.8</sub>	47.866	29	53
15	Ni <sub>50.1</sub> Mn <sub>30.7</sub> Ga <sub>19.2</sub>	32.885	1	60
16	Ni <sub>46.6</sub> Mn <sub>34.1</sub> Ga <sub>19.3</sub>	38.766	43	70

Table 1.  
Summary of Sample Properties

Samples 3 and 7 did not show a distinct martensite transformation during the magnetization vs. temperature tests. However, the behavior they exhibited was not common to the rest of the samples. The different behavior suggests that these samples may be martensite, but not show an abrupt transformation. Both of these samples have low Curie temperatures so it is possible that the transformation may occur at a temperature higher than the Curie temperature. If this is the case, the method used to determine martensite temperature in this study will not be effective in determining the transformation temperature of these samples.

## Chapter 5

### Discussion

In processing the samples, several variables in addition to composition can affect the properties. For example, melt temperature and time can increase the loss of high vapor pressure elements, such as gallium and manganese. Cooling rate may also affect grain growth, macro-phase segregation for some off stoichiometry samples, and internal stress. Effort was made to ensure the processing parameters varied slightly between samples. The temperature of the molten metal was not constant for all samples. The temperature varied from 1300 °C and 1400 °C. The time the samples were molten was not constant either. The samples were molten from 3 to 5 minutes to accommodate apparent differences in homogeneity of the melt. The goal during processing was to keep the temperature as low as possible to avoid vaporization of the material. Some of the samples were not homogeneous throughout the length of the ingot due to differences in preparation. However, EPMA showed that all but two the samples were homogenous on surfaces perpendicular to the length of the ingot. The two samples that were found to be inhomogeneous had pockets of nickel which indicates that the samples were not heated to high enough temperatures or for long enough times. These two variations have made it difficult to find the trend of how the final compositions vary from the intended compositions. In general, samples can be controlled to within one atomic percent of their intended composition after induction melting. For more precise compositions, the

processing conditions will have to be controlled more carefully to ensure proper homogenization and prevent vaporization. Another way to control the homogeneity of the samples is to crush the ingots and melt them a second time.

Trends in properties can be established by plotting the properties of the samples as a function of their composition. Samples close to the composition of  $\text{Ni}_{50}\text{Mn}_{30}\text{Ga}_{20}$  have the highest saturation magnetization. Samples that vary greatly from this composition have lower magnetization and two samples are paramagnetic. Samples low in gallium and high in nickel are paramagnetic. The magnetization of samples increases as nickel content rises and manganese content decreases for near constant gallium concentrations. Figure 5.1 shows the magnetization as a function of composition.

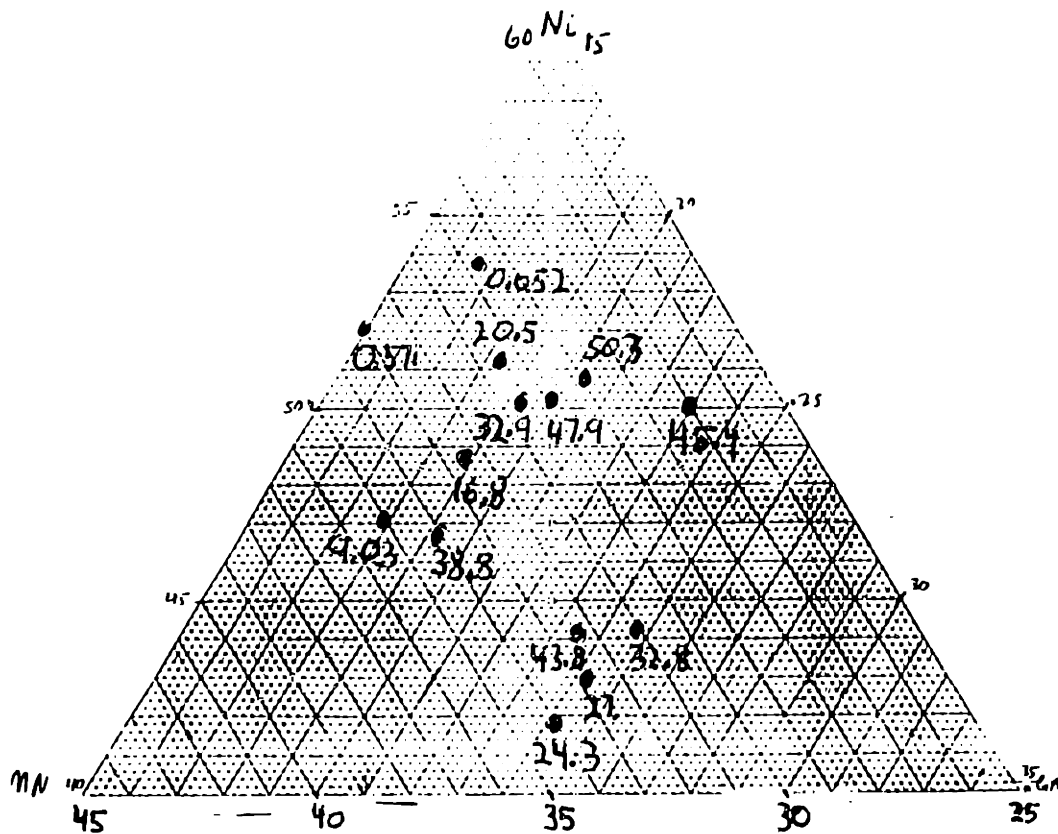


Figure 5.1  
Magnetization as a function of composition

Figure 5.2 shows martensite temperature as a function of composition.

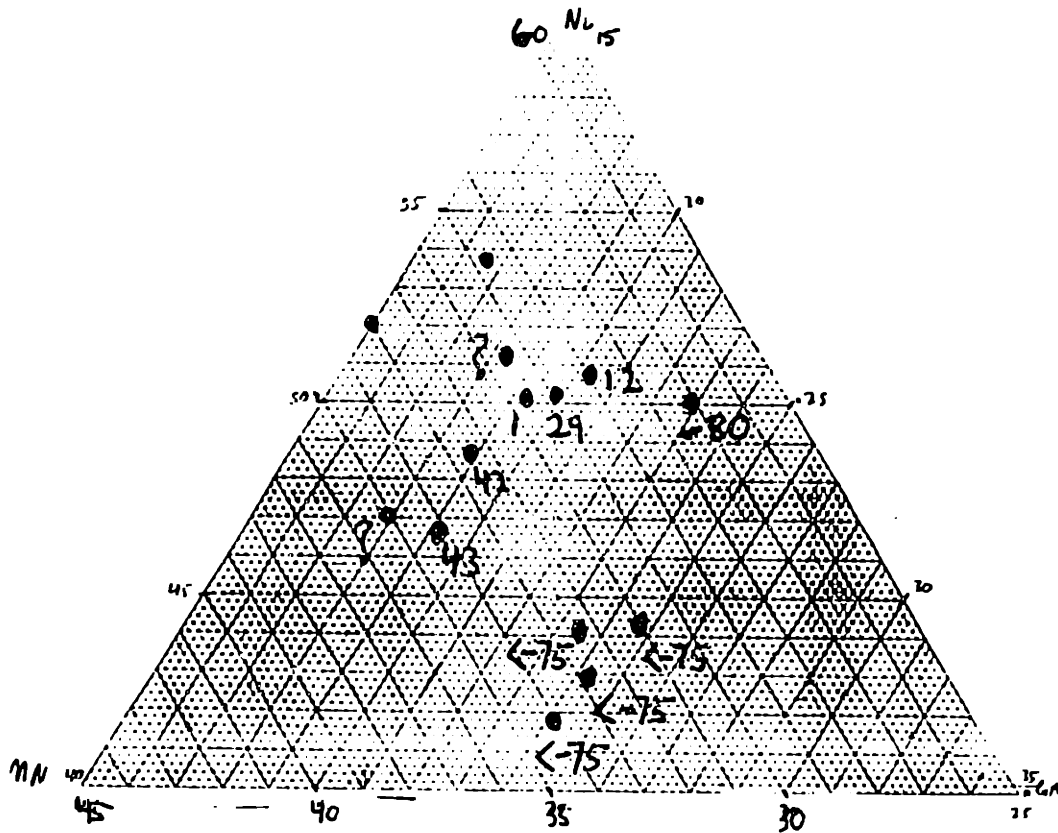


Figure 5.2  
Martensite temperature as a function of composition.

Martensite transformation temperatures are near room temperature for a band of compositions. Samples with gallium content between 19 and 22 atomic percent exhibited martensite temperatures near room temperatures. The highest martensite transformation temperatures were found in samples in this band that had higher manganese contents and lower nickel contents. The martensite temperature decreased sharply on both sides of this band. Samples with gallium content lower than 19 atomic percent or higher than 22 atomic percent did not show martensite transformations above  $-75^{\circ}\text{C}$ . It is possible that the stress the sample is subjected to changes the martensite transformation temperature.

High transformation temperatures may only be seen in the narrow band because outside the band may be multi-phase compositions which have high internal stresses. Examination of a phase diagram would be useful in determining why high martensite temperatures are only seen in the narrow region. Curie temperatures do not vary with composition as sharply as the martensite temperatures. Figure 5.3 shows Curie temperature as a function of composition.

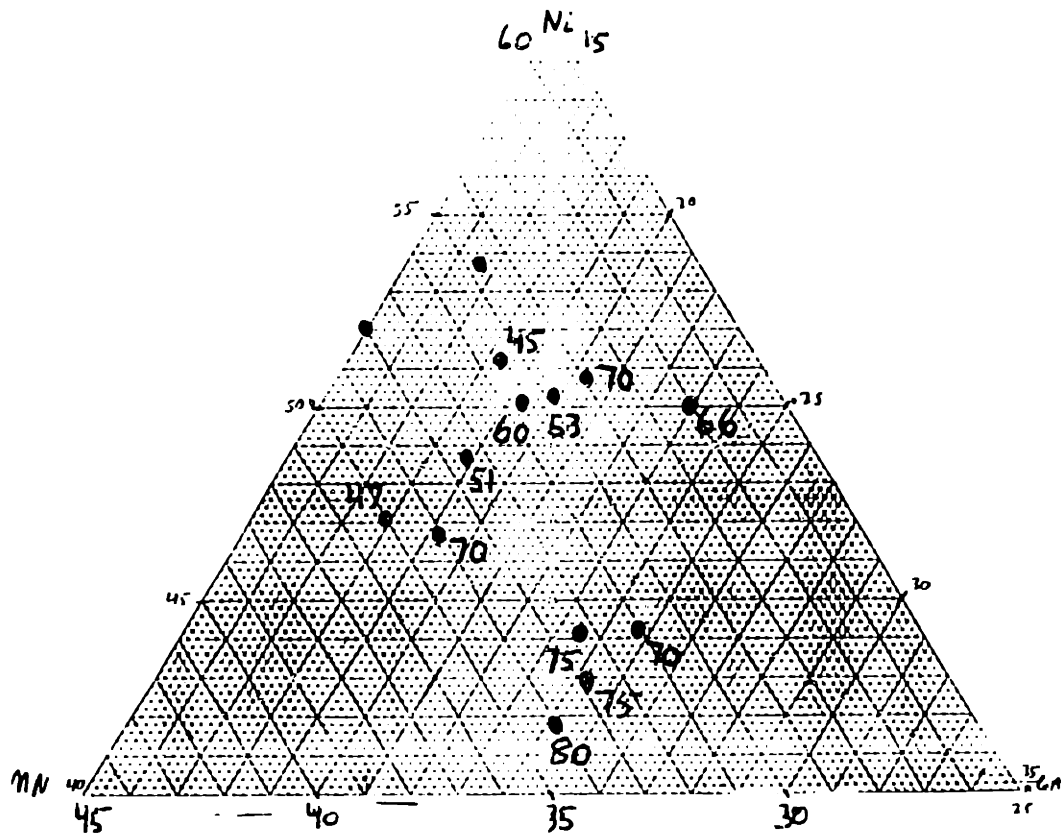


Figure 5.3  
Curie temperature as a function of composition

A broad ridge of high  $T_C$  compositions is found to run parallel to the narrow band of high  $T_M$  compositions. Curie temperature apparently is not a parameter that is very sensitive to composition in this range.



The magnetostriction of the samples was less than reported in single crystals. This is to be expected because these samples are polycrystals with no significant degree of texture. The single crystals can strain in a coherent way whereas the various grains of the polycrystals strain in ways that are incompatible. This causes the polycrystals to have lower amounts of strain because some of the strain can be accommodated at the grain boundaries of the samples. However, this does not explain why some of the samples exhibited no magnetostriction in the martensite phase.

## **Chapter 6**

### **Conclusions**

Property control of Ni<sub>2</sub>MnGa samples can be achieved through variations in composition. Compositions that exhibit relatively high martensite transformation temperatures have been found. In particular, samples 2, 4, and 16 look attractive for further study. Attempts should be made to increase the grain size and induce texture in these samples, perhaps by mechanical deformation and float zone refinement. Based on our present knowledge of single crystals, these compositions should show large magnetic field induced strains. In addition, magnetization varies greatly with composition. Extrapolating trends found in this thesis will guide future studies to the composition that maximizes both properties.

Polycrystalline samples probably will not be effective for use as actuators unless they are highly textured. Magnetostriction in the polycrystals is much lower than that found in the single crystals. Many polycrystalline samples may not show any magnetostriction because the strains will be accommodated at the grain boundaries. Future studies should examine the difference in properties between single crystals and

polycrystalline samples of the same composition to determine the effect of crystal structure on performance. The processing of the samples should be monitored carefully to find the best processing method.

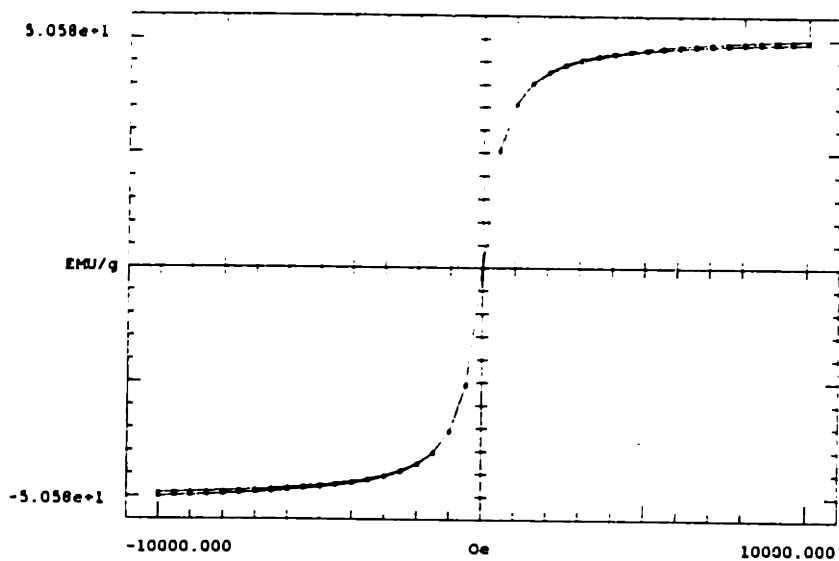
Future experiments will have to examine the frequency response properties of the material. Rapid frequency response is very important for actuator materials. So far, there has been no published work about the frequency response of nickel-manganese-gallium. A phase diagram should be composed for this compound to determine where single phase regions exist. Currently, there is not a phase diagram available for nickel-manganese-gallium. Another source for improvements in the properties is mechanical biasing. Pre-stressing the samples will align the twin variants which may yield larger magnetostrictive strains. This is typically done in Terfenol-D actuators [8].

## References

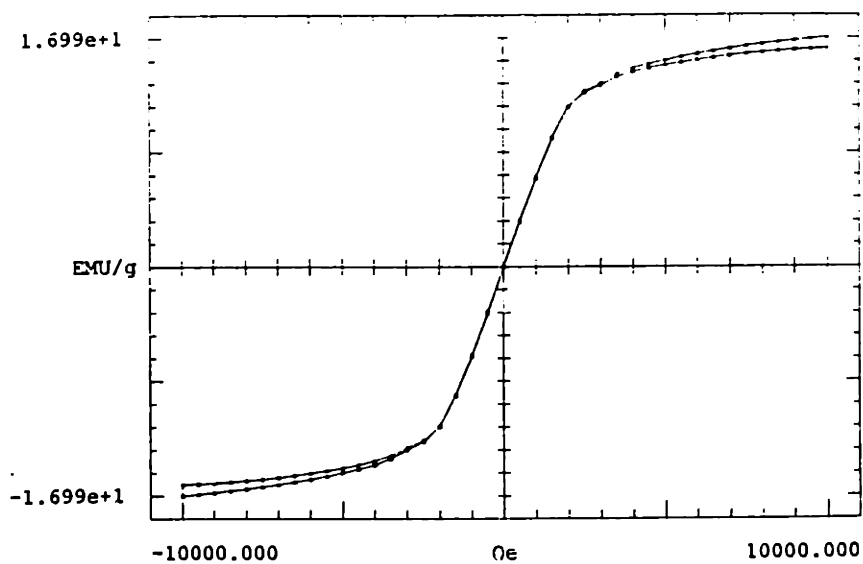
1. K. Ullakko, *Journal of Materials Engineering and Performance*, **5**, 405.
2. K. Ullakko, P. T. Jakovenko, and V. G. Gavriljuk, *Proceedings of Symposium on Smart Structures and Materials*, 1996, SPIE- The International Society for Optical Engineering, Vol. 2715. San Diego, February 26-29, 1996.
3. P. J. Webster, K. R. A. Ziebeck, S. L. Town, M. S. Peak. *Philosophical Magazine B*, **49** (1994), 295.
4. V. V. Kokorin and V. V. Martynov, *Fiz. Met. Metalloved.*, **9** (1991), 106.
5. Ullakko, K., J. K. Huang, C. Kantner, R. C. O'Handley, and V. V. Kokorin. *Applied Physics Letters*, **69** (1996), 1967.
6. V. A. Chernenko, E. Cesari, V. V. Kokorin, and I. N. Vitenko, *Scripta Metallurgica et Materialia*, **33** (1995), 1239.
7. R. D. James and Manfred Wuttig. Submitted to *Phil. Mag. A*.
8. A. E. Clark, J. P. Teter, and O. D. McMasters, *J. Appl. Phys.*, **63** (1988), 3910.

# Appendix A

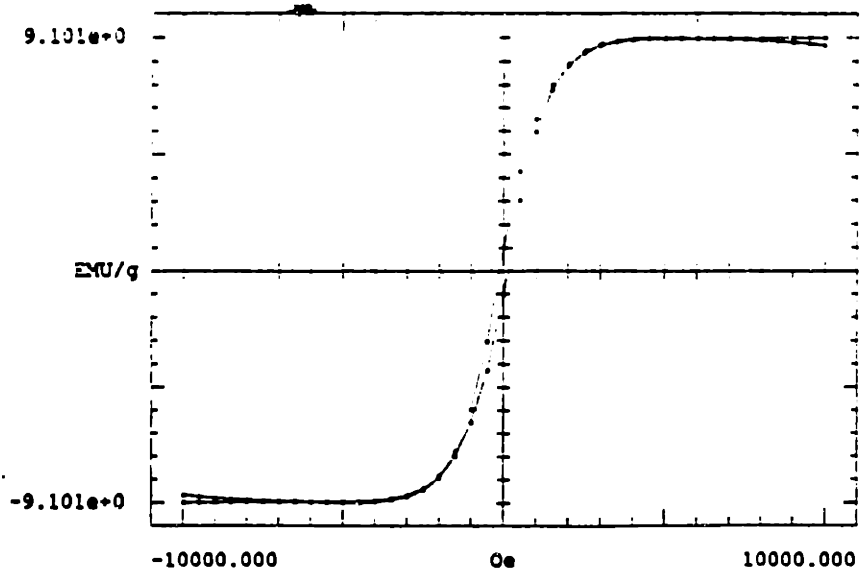
Room temperature magnetization vs. field graphs of all samples tested.



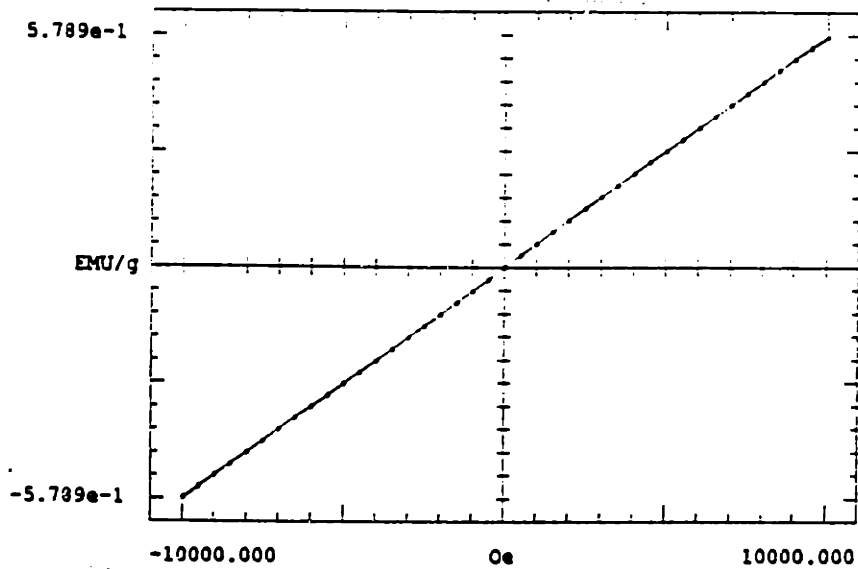
sample 1



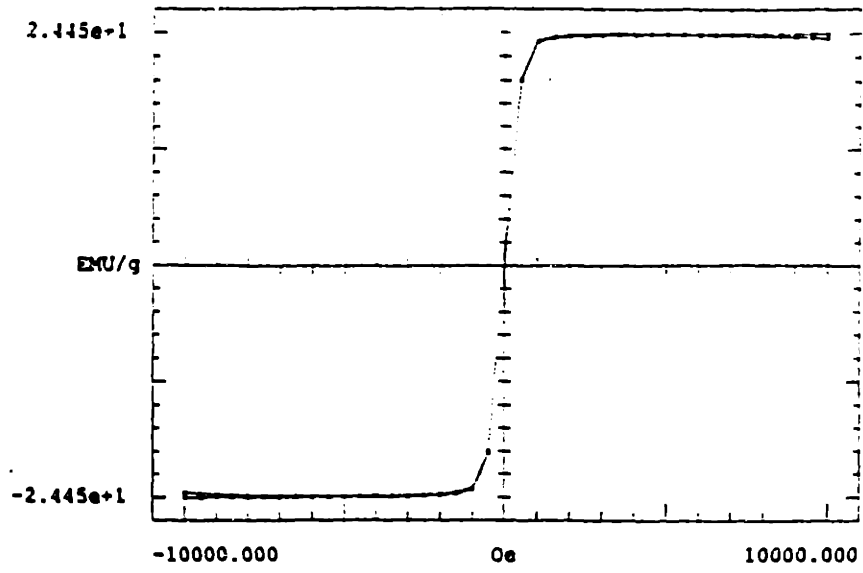
sample 2



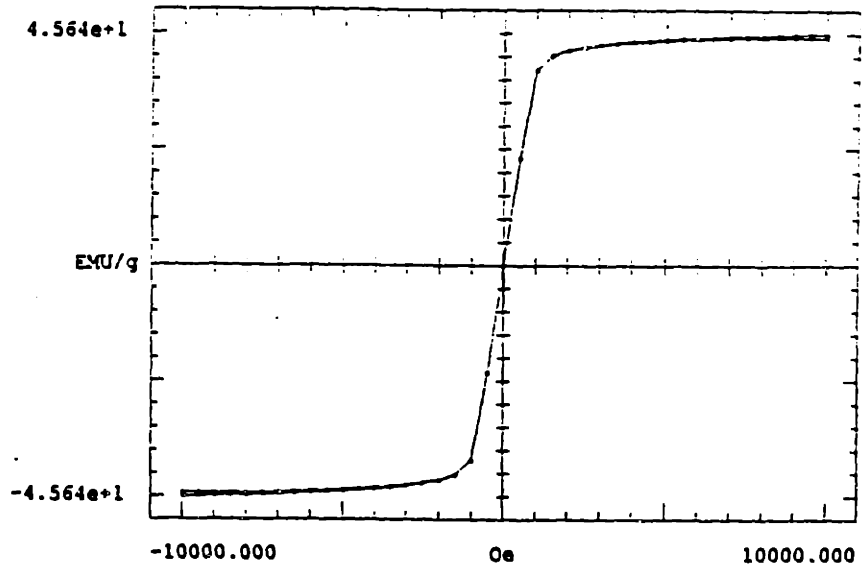
sample 3



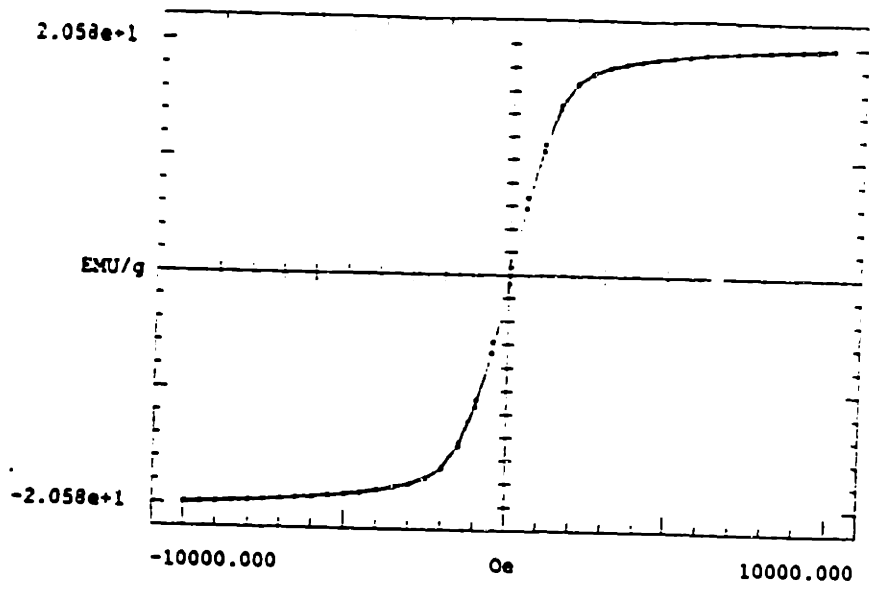
sample 4



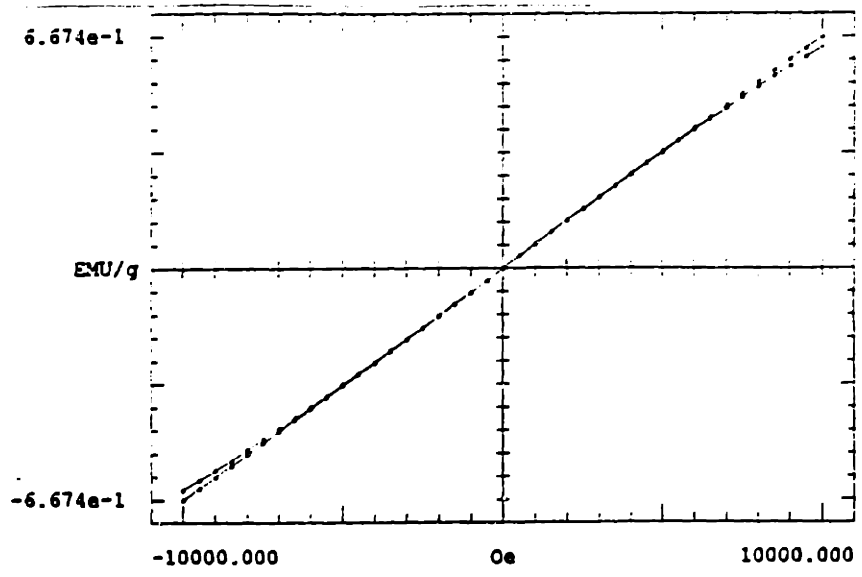
sample 5



sample 6

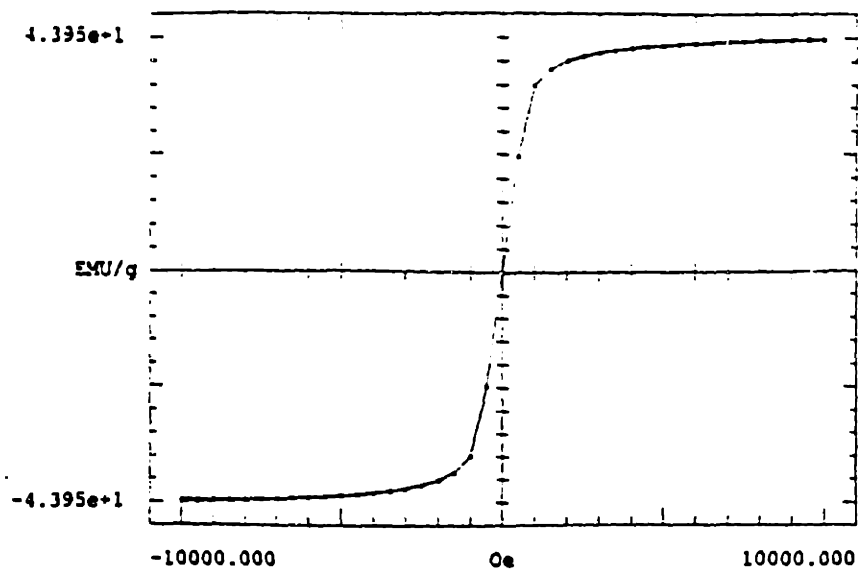


sample 7

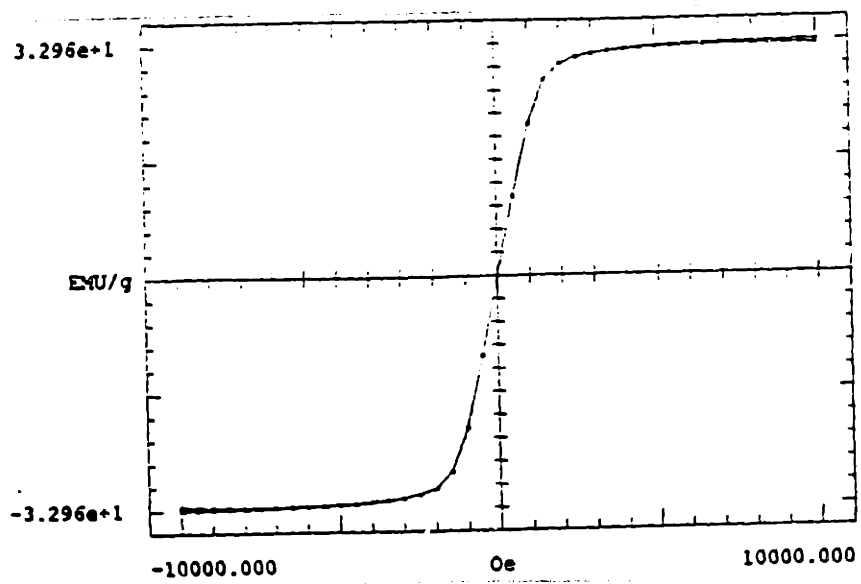


sample 8

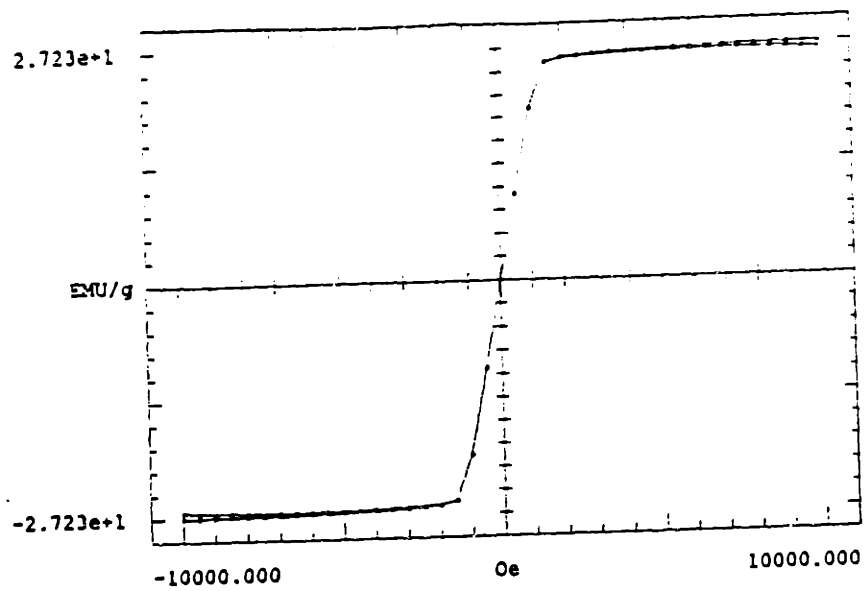




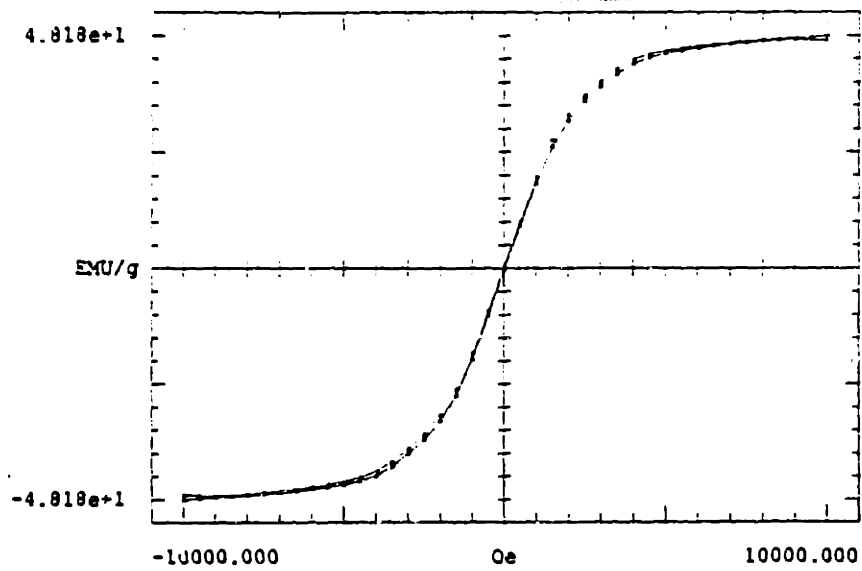
sample 9



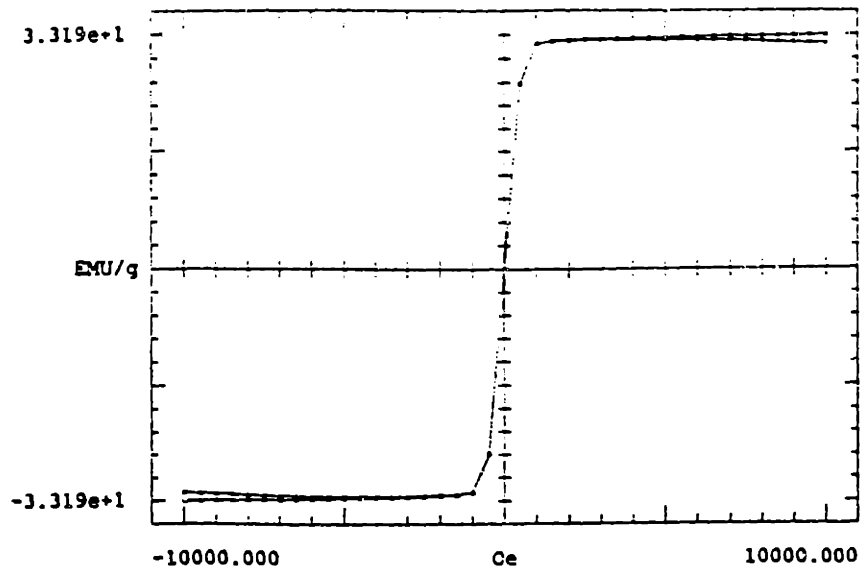
sample 11



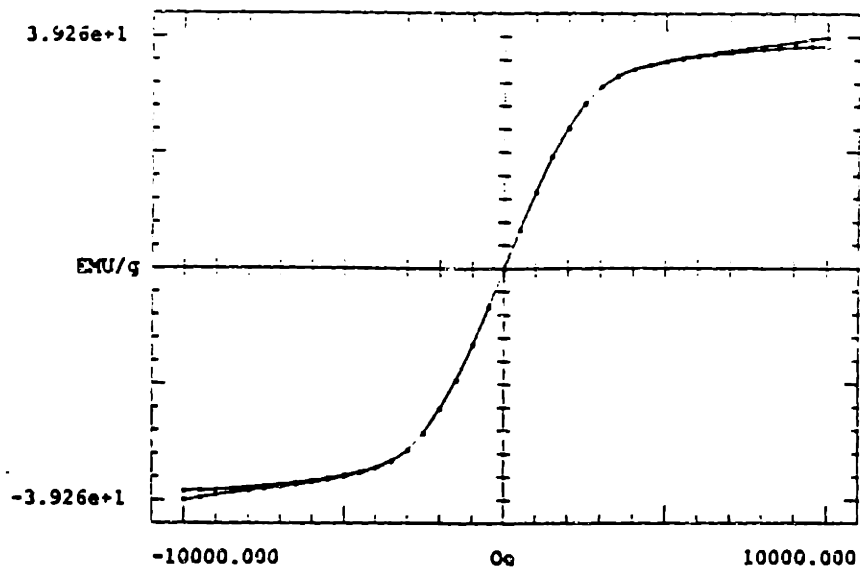
sample 12



sample 14



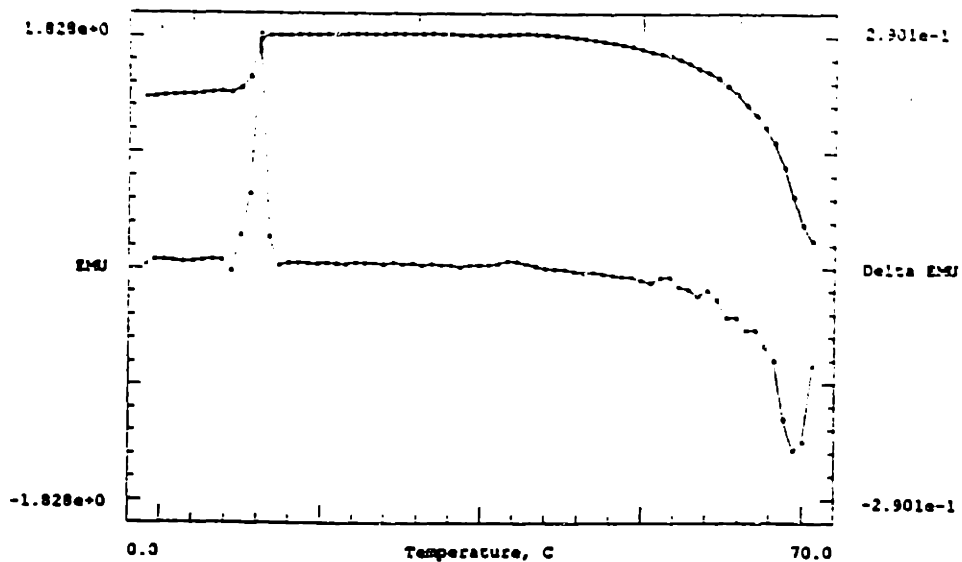
sample 15



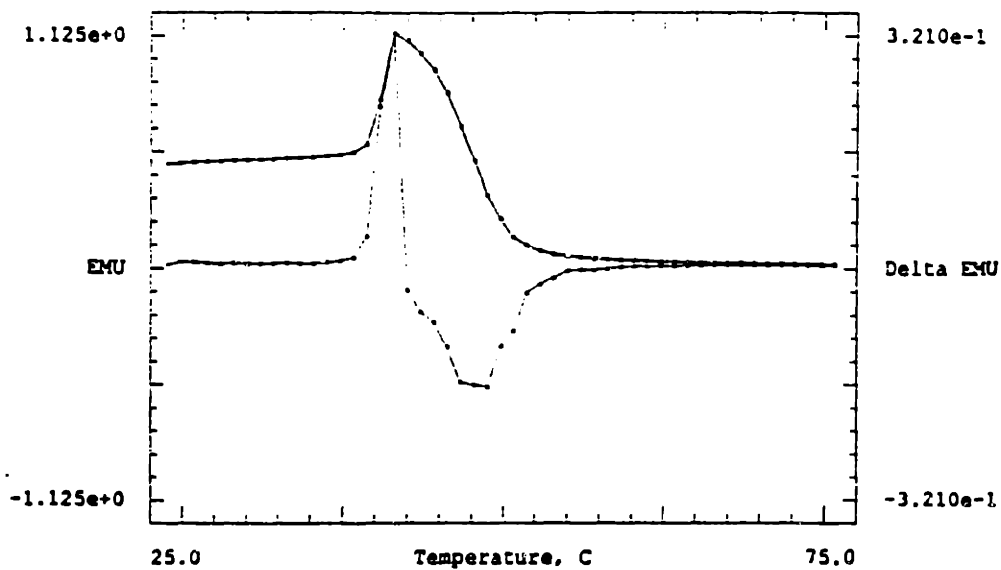
sample 16

# Appendix B

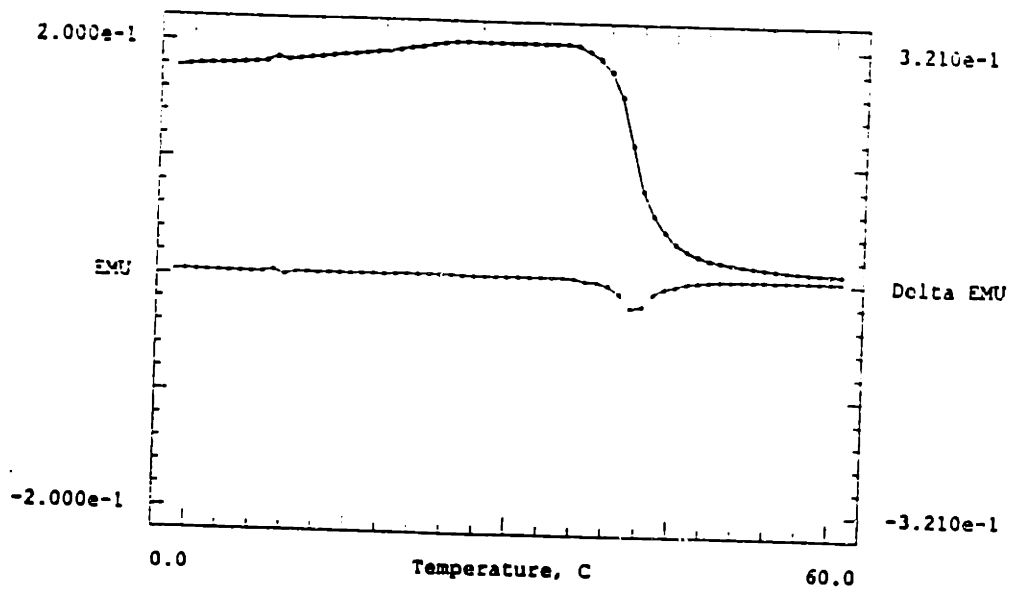
## Magnetization vs. temperature in 500 Oe field



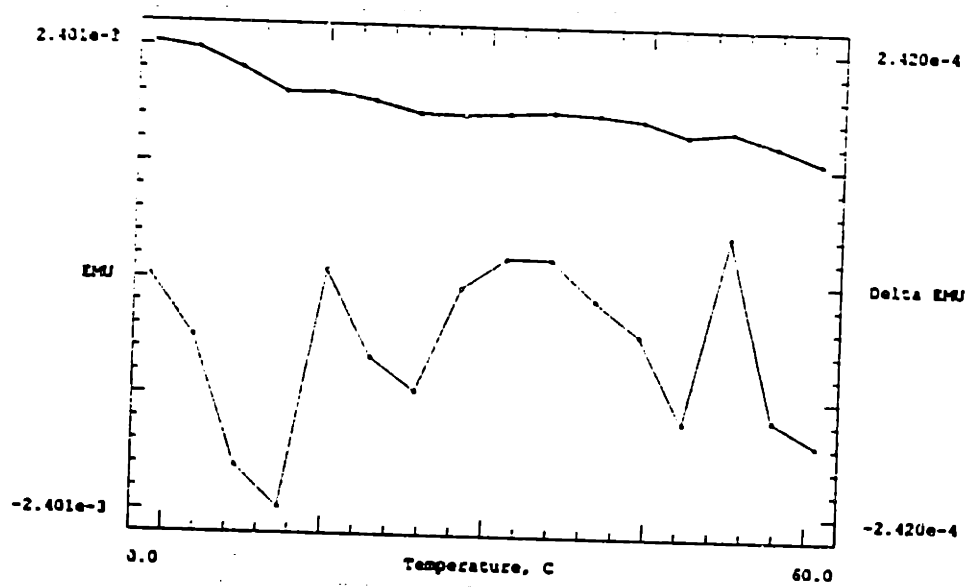
sample 1



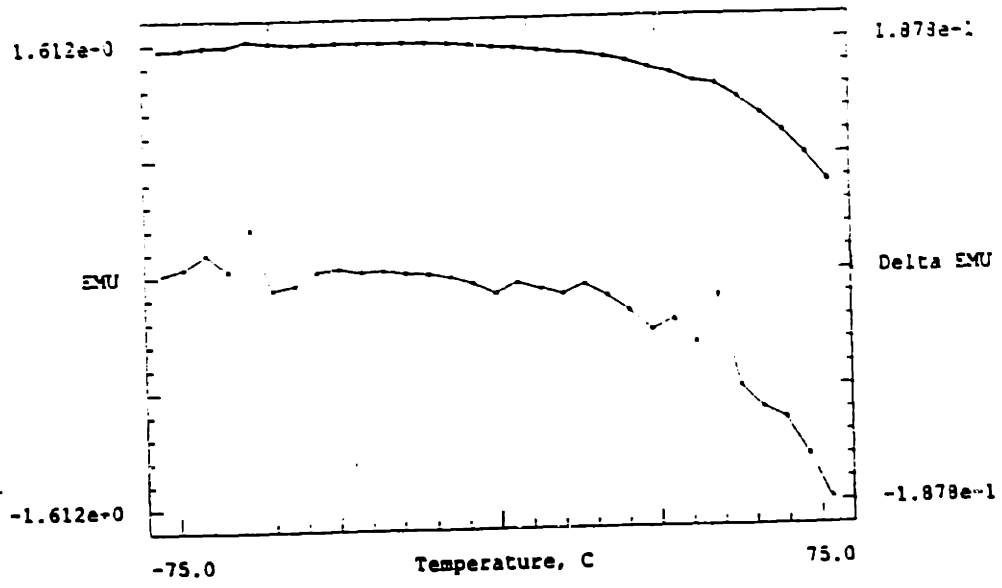
sample 2



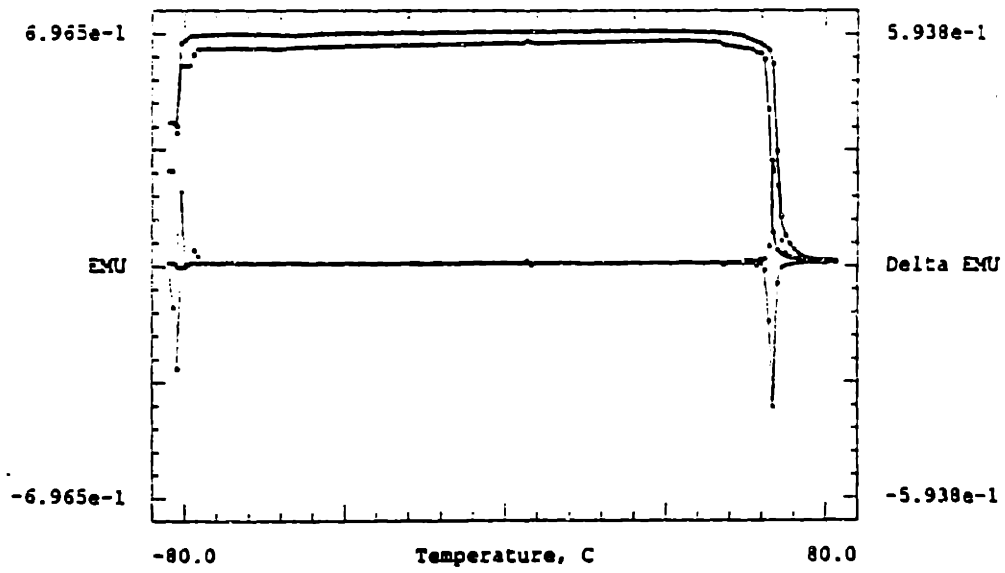
sample 3



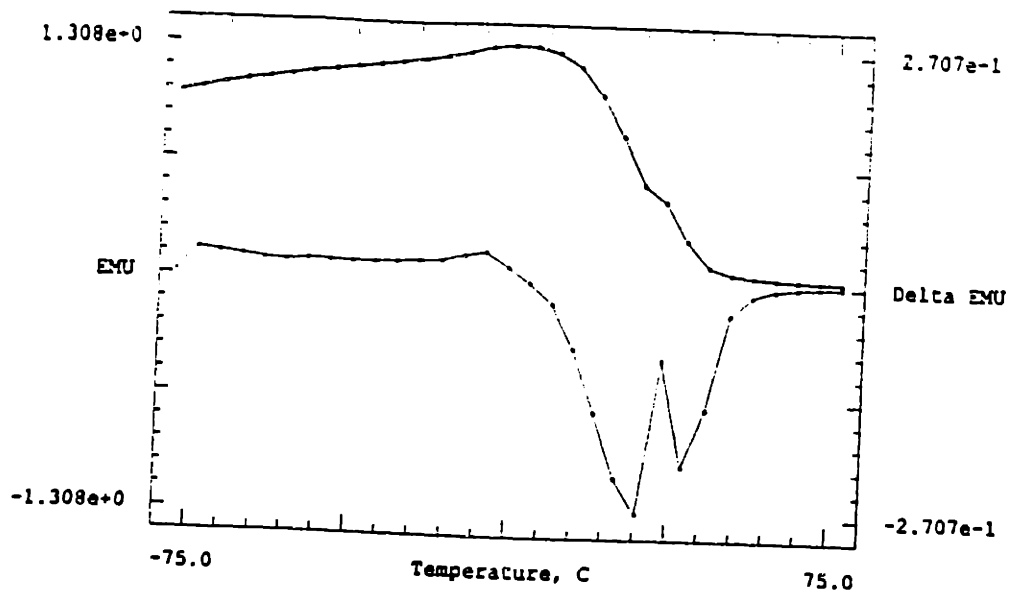
sample 4



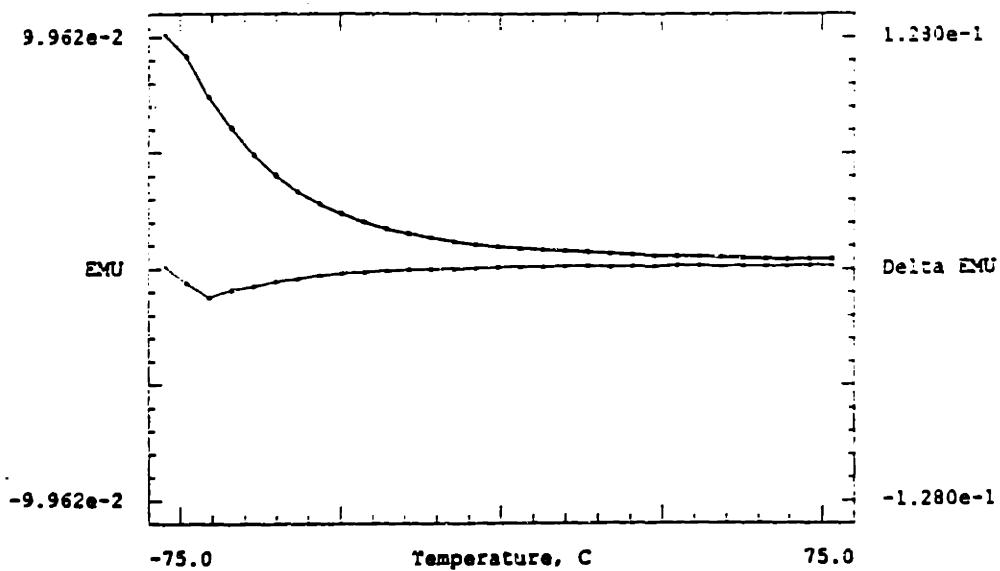
sample 5



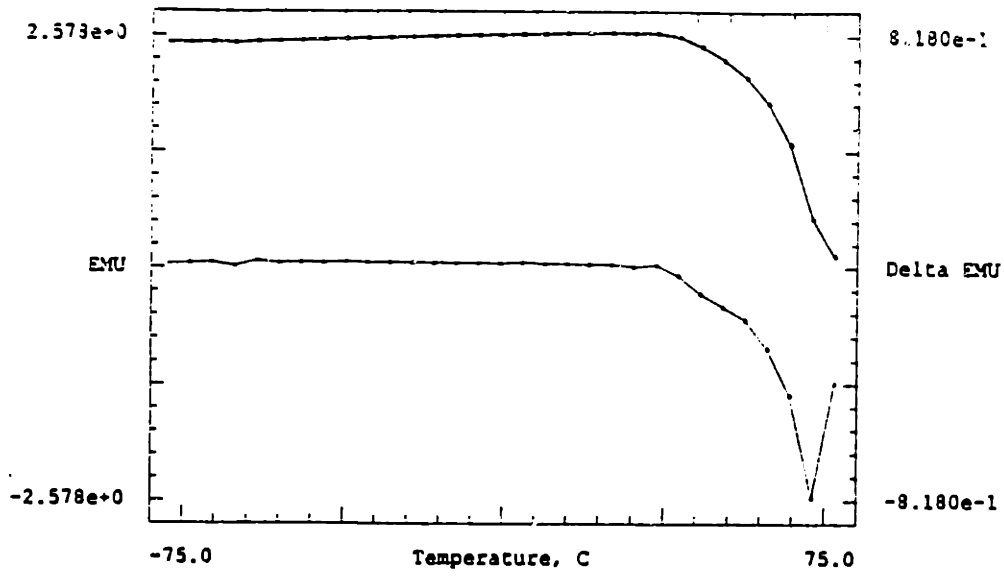
sample 6



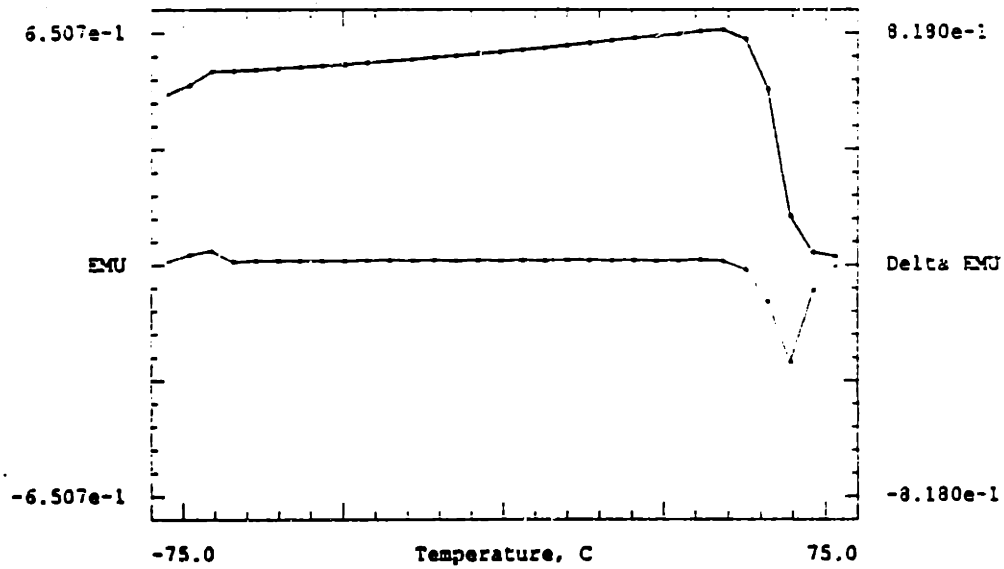
sample 7



sample 8

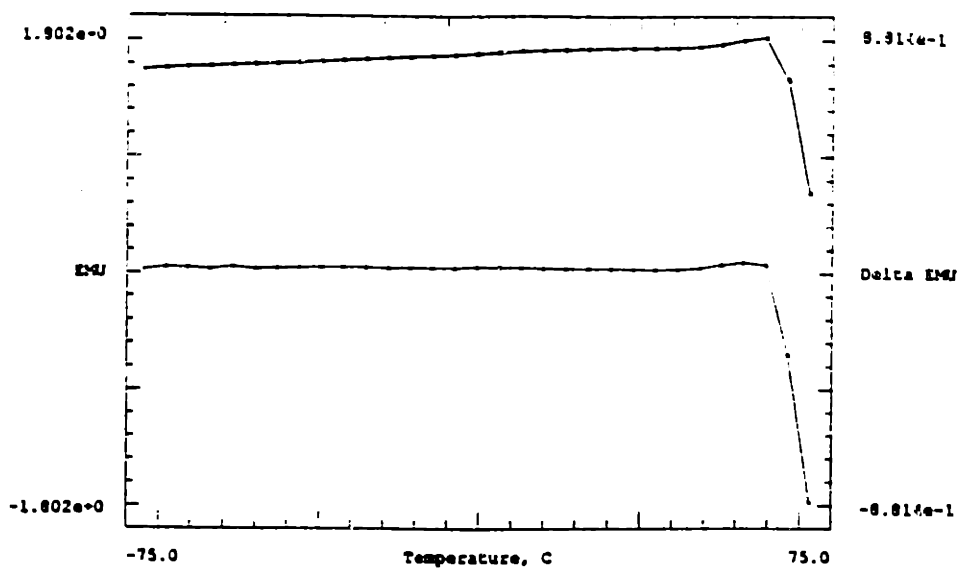


sample 9

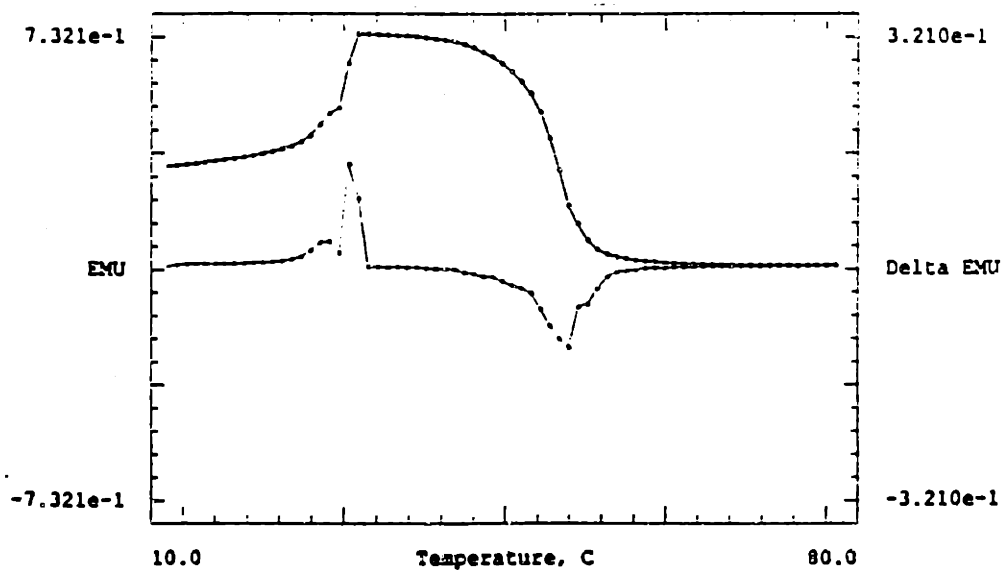


sample 11

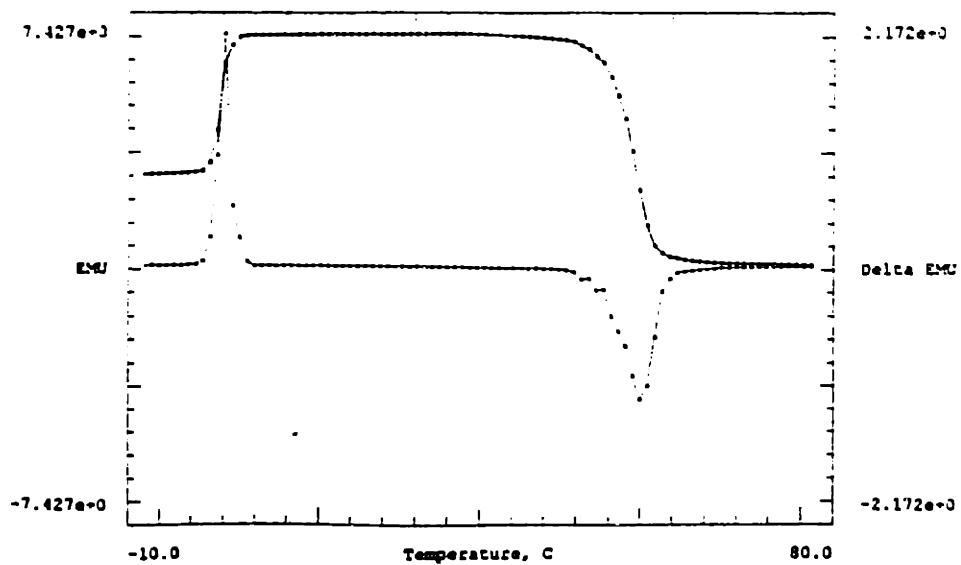




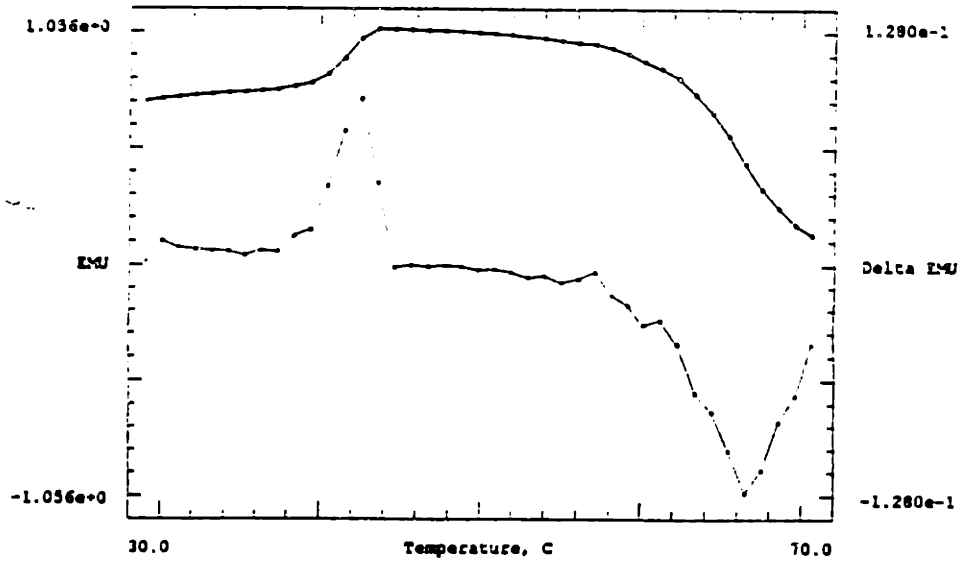
sample 12



sample 14



sample 15



sample 16